Silicon (2024) 16:345–366
https://doi.org/10.1007/s12633-023-02662-6

RESEARCH

Recent Advances Ultra-Porous Drug Nano-Carriers: Synthesis and Targeting Approaches

Mayssa Abdel Hady[1]

Received: 12 July 2023 / Accepted: 3 September 2023 / Published online: 23 September 2023

Abstract

Mesoporous silica has attracted increasing interest due to the pandemic spreading of the viral infection in recent years. These smart materials have many advantages as high loading capacity, high surface area, and unique morphology making them great materials for smart drug carriers. In this review, I summarized the synthesis of Ultra-Porous Drug Nano-Carriers in recent years. Factors affecting (mesoporous nanoparticles) MSN Synthesis as surfactants, Co-surfactants, and solvents were mentioned in the full description and targeting approaches. Types of silica nanoparticles such as Mesoporous SBA-1 silicas, Mesoporous SBA-2 silicas, and hybrid mesoporous materials are also shown in a detailed manner. Future research efforts are also highlighted for AI-based techniques aimed at more accurate tissue engineering prediction and operation optimization in drug carrier-based processes.

Keywords Mesoporous silica · Drug carrier · RSM · MSN · Artificial intelligence · Machine learning

1 Introduction

Porous nanostructures are a unique class of materials with pores or holes at the nanoscale and demonstrate various physicochemical characteristics [1]. Their content, size, and shape all affect these characteristics [2]. Porous nanomaterials offer unique features compared to uniform particles of the same size because of their unoccupied spaces, such as low densities [3–5], broad dynamic surfaces, low refractive coefficients, excellent permeabilities, excellent effectiveness, and thermal and acoustic resilience [6, 7]. The previously stated properties of porous nanostructures are determined by the ratio of free-space pores to the total volume of a material dubbed porosity [8, 9], in this category, a pore connected to the free surface of a substance is called an open cell. Materials having these open cells may be used for filtration, membranes, separation, chemical processes, functioning as catalysts, and chromatography, among other things [10]. Closed cells are pores far from a composition's free surface and do not contribute to any chemical applications, even if they boost the materials' thermal and acoustic resistance and reduce their weight [7, 11]. Several types of pores exist, including spherical, cylindrical, grooved, and hexagonal forms. Numerous porous nanoparticles on the market have a wide range of characteristics, architectures, and uses [12]. One of the key advantages of mesoporous silica nanoparticles (MSN) is its ability to provide controlled and sustained release of biologically active substances [13]. Their porous structure allows for controlling the release of drugs over time, which can be critical for optimizing therapeutic efficacy and minimizing side effects. This is achieved by controlling the pore size and surface chemistry of the MSN, which can be tailored to optimize drug release kinetics. Another advantage of MSN is its ability to enhance targeted drug delivery. The surface of MSN can be functionalized with specific ligands or antibodies that target specific cell types or tissues, allowing for enhanced drug delivery to the anticipated site of action. This can boost the effectiveness of the drug while minimizing off-target effects. Furthermore, it is biocompatible and non-toxic, making it a safe option for drug delivery. It is also highly chemically stable, ensuring the drug remains stable during storage and delivery weight [7, 11, 14, 15].

Lastly, MSN can be used to monitor and control biological processes. For example, it can serve as a platform for imaging and sensing applications, allowing real-time exploration of drug release and biological responses to the

✉ Mayssa Abdel Hady
ma.abdel-hady@nrc.sci.eg

[1] Pharmaceutical Technology Department, National Research Centre, El Bohouth Street, Cairo 12622, Egypt

delivered drug. Overall, MSN has several advantages over traditional drug delivery methods, making it a promising platform for drug delivery and biomedical purposes. Therefore, this review's fundamental objective is to inform readers about the current exploits of MSN as a nano-catalyst carrier for drug delivery. The fabrication of this kind of nano-catalyst and its catalytic system has been made conceivable by revolutionary techniques up to this point.

2 Types of Silica Nanoparticles

2.1 SBA-1 Silicas

Mesoporous SBA-1 silicas feature a 3-dimensional cubic shape with Pm3n geometry and open porosity of the 3D cage type interconnected by open windows. The materials feature distinctive topographical features, such as pores with dimensions ranging from 2.1 nm to 2.6 nm and a particular area of the surface of 1200–1450 m^2/g [16, 17]. The 3-dimensional porosity structure provides multiple places for adsorption and is resilient to obstruction. Because SBA-1's cubic design is more durable than silicas with hexagonal shapes, it is regarded as excellent catalyst support. The fabrication of SBA-1 materials was complex, Huo et al. [18] and co-authors attempted to synthesize SBA-1 materials in a different and innovative manner.

2.2 SBA-2 Silicas

SBA-2-type silicas are less widely recognized than SBA-1-type silicas. The previous example features a 3D pore network with hexagonally and cubically packed (hcp and ccp, respectively) spherical holes linked by cylindric channels [19–21]. It is essential to highlight that the SBA-2 and SBA-12 silicas possess the same 3D hexagonal structures and P63/mmc symmetry. Triblock copolymer has been utilized as a mesoporous structure guiding compound to achieve the latter [19, 22]. Only the hexagonal pore system was discovered in SBA-2 silica after its first synthesis; an in-depth study subsequently confirmed the existence of the cubic pore structure [23].

2.3 HMM Type Materials

A recently developed category of mesoporous organic–inorganic hybrid materials, referred to as hybrid mesoporous materials and symbolized by an abbreviation HMM, was first synthesized in 1999 by Inagaki et al. [24]. Due to the presence of organic and inorganic groups in their structures, the materials fall under the Periodic Mesoporous Organosilicas (PMOs), which are connected by covalent bonds to form a hybrid organic–inorganic lattice [24]. The group of HMM is separated into the HMM-1 and HMM-2 subgroups. Their assembly is composed of silica groups (Si_2O_3) and uniform ethyl fragments (-CH_2-CH_2-), which create a network that is connected by covalent connections [25–27]. The permeability makeup of these substances differs essentially from the one found in mesoporous materials, which consist of an inorganic lattice onto which organic modifications are grafted. According to HMM-1 and HMM-2, hexagonal rods and spherical particles have well-defined morphologies and a highly organized mesoporous structure, respectively [25]. The same chemicals, 1, 2-Bis (trimethoxysilyl) ethane (BTME), and hexadecyltrimethylammonium chloride (ODTMACl), were used in the fundamental circumstances to create these two compounds. The synthetic mixture's components' synthesis temperature and molar ratio controlled their structural composition. The consistent pores in the materials were opened by extracting the surfactant using a solvent, and the ordered structure was not compromised. Hydrothermal stability was a property of the materials [24, 28]. The HMM-1 model has been demonstrated to possess a hexagonal 2-dimensional structure with p6mm symmetry, characterized by 1D pores of sub-10 nm sizes and an extensive surface area of up to 1000 m^2/g. The utilization of HMM-1 as a prototype for manufacturing nanoparticles of metal and nanowires was attributed to its distinctive features [29, 30]. Similar purposes have been identified for HMM-2 of a 3D P63/mmc symmetry structure [31].

3 Preparation of Mesoporous Silica Nanoparticles

Stober was the developer of the system of chemical reactions for producing spherical monodisperse micron-sized silica particles [32, 33]. Surfactants serve as structure-directing agents when producing mesoporous materials (Fig. 1) [34]. However, the main three basic steps of synthesis are (a) sol–gel process, (b) The utilization of surfactants as structure-directing agents to synthesize mesoporous materials and (c) the execution of a modified Stober method under dilute conditions for the manufacturing of cylindrical nanoparticles are two critical techniques in materials science [33, 35–38]. The hydrolytic sol–gel method, in which silicon alkoxide predecessors are hydrolyzed and compacted under acidic or alkaline catalysis, is the most employed approach to manufacturing silica NPs, even if there are other techniques to generate MSNs [35].

3.1 The Sol–gel Method

Polycondensation occurs adjacent to surfactant particles to create an oxide system from precursors, which illustrates the structure. The network then generates a colloidal solution

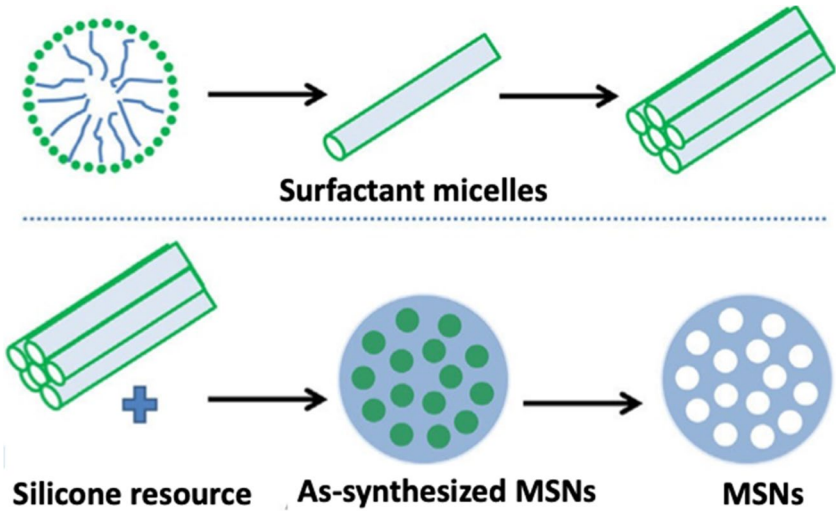

Fig. 1 Schematic diagram showing the preparation of MSNs [34] permission from Elsevier

(sol), which relies upon the reaction conditions (the rate at which varying reaction factors carry out polycondensation processes). It gradually generates a gel or discrete particles [35, 36]. Mono-dispersed spherical silica particles are created when the solution is highly diluted [32]. The generation of NPs and the ensuing mesostructure of the material are significantly influenced by temperature, surfactant type, and concentration (Fig. 2) [39]. Hydrolysis produces silica monomers, which interact to co-assemble and produce mesostructured nanocomposites. To create the finished product, MSN, these nanocomposites are calcined [40]. Besides calcification, other techniques include dialysis, extraction of supercritical CO_2 fluid, liquid-phase calcination, microwave-assisted template removal, acid treatment, ozone therapy, and liquid-phase calcination [41].

The Templating Method Using a template, the hollow porous framework is generated. (Structure-directing agent). Endo-template (soft matter templating) and exo-template are the two sub-methods of this methodology. (Complex matter templating). The exo-template technique employs a porous solid as a template and fills the empty spaces with an inorganic precursor that converts when subjected to suitable pH and temperature conditions [42]. In the endo-template strategy, an organized mesoporous material can be produced using a surfactant as a template; no complex template solid is needed [43, 44].

3.2 The Microwave-assisted Method

Heating enabled by a microwave is more rapid than conventional heating. Furthermore, homogeneous heating of the sample encourages the development of uniform nucleation centers in the precursor solution when silica monomer condensation over the template first starts [45]. This method delivers high localized heating that might exceed the reaction vessel temperature. Thus, this one is the best way to produce mesoporous materials [42]. Used for rapidly synthesizing various materials, such as ceramic oxides and porous materials [46].

Concurrently, improved mesoporous silica columns were generated via a polycarbonate membrane with a pore diameter of 0.2 m within an empty receptacle. A 1 mL quantity of a pre-existing blend containing pluronic P123 co-polymer,

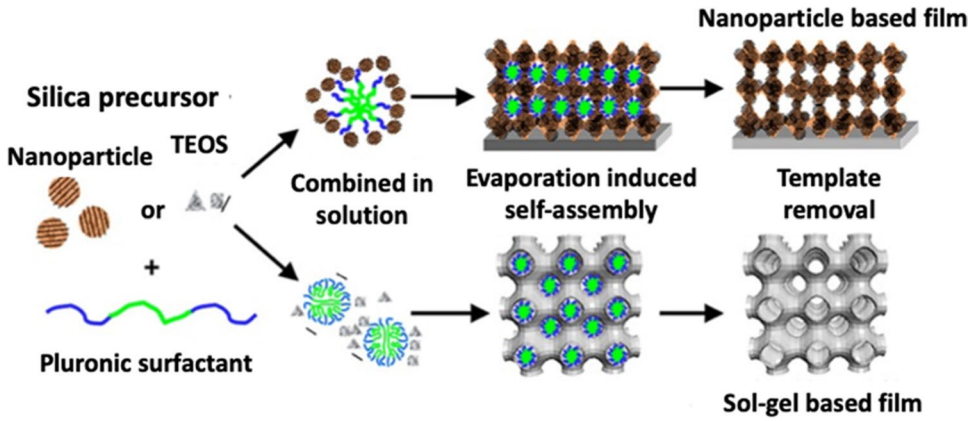

Fig. 2 Illustration of Sol–gel technique for MSN synthesis [39] Permission from American Chemical Society

hydrochloric acid (HCl), ethanol, and TEOS (Tetraethyl orthosilicate) was added to the receptacle. Subsequently, the case was positioned within a larger vessel, sealed, and subjected to microwave irradiation at 40°C. Silica rods featuring pores measuring 6 nm in size and 200 nm in diameter were successfully synthesized, with each rod starting from a single polycarbonate membrane pore. This approach produces well-structured pores and is speedier for production than the conventional sol–gel method [47].

3.3 Self-assembly Caused by Evaporation

In the Evaporation-Induced Self-Assembly (EISA) process, solvent evaporation causes a change in each component's concentration at the liquid–vapor interface. The chemical solvent is released while the material passes through a drying compartment or furnace at 400 °C, where silica and surfactant immediately form micelles. Causing a liquid–crystal mesophase to develop, which then spreads outwardly from the liquid–vapor border to the droplet's center, producing MSN [48]. Jing et al. used a cellulose nanocrystal mixture and TEOS as a precursor for silica at pH 2.4 in the EISA procedure to make mesoporous silica film (MSF) [49].

3.4 The Technique of Chemical Etching

Mesoporous structures can be generated without a requirement for a template (soft or hard) by utilizing a selective etching agent that could be either elementary or acidic in nature (Fig. 3) [50]. This method generates hollow-type mesopores with controlled pore size based on structural distinctions between a silica core/mesoporous silica core and shell [42]. By using mesoporous silica as the shell and inorganic nanocrystals (such as Au, Fe_2O_3, and Fe_3O_4 NPs) as the core, this approach can be used to construct a wide variety of heterogeneous hollow nanostructures. Traditional approaches, such as templating techniques, have displayed only minor success in regulating mesoporous materials' particle/pore shape and dimension [51].

Nevertheless, in the chemical etching process, a homogenous templating technique known as "structural difference-based selective etching" is used to construct the porous core/shell structure. By selectively etching the interior of the building while mostly keeping the outside shell intact, this technique turns the design into a hollow one. By using the proper etching agent, this is accomplished [42].

3.5 Sol–gel Method with Assistance from Electrochemistry

The investigation of electrochemistry as a further method for producing MSN using the technique known as sol–gel depends on the hypothesis that applying electricity causes a chemical change. An electrode coated in the precursor mixture containing the surfactant that is employed is as a cathodic voltage to produce the hydroxyl ions essential for the micellar composition and to trigger the polycondensation response of the earlier prepared in situ silica monomers using catalytic hydrolysis to assemble the MSF layer over the electrode being exploited. The thickness of the MSF can be changed over time at the best operating potential by varying the electrode position's duration [52]. This technology is suitable for industrial MSN production because it allows for straightforward, quick, and affordable to produce MSN at the gram size [53].

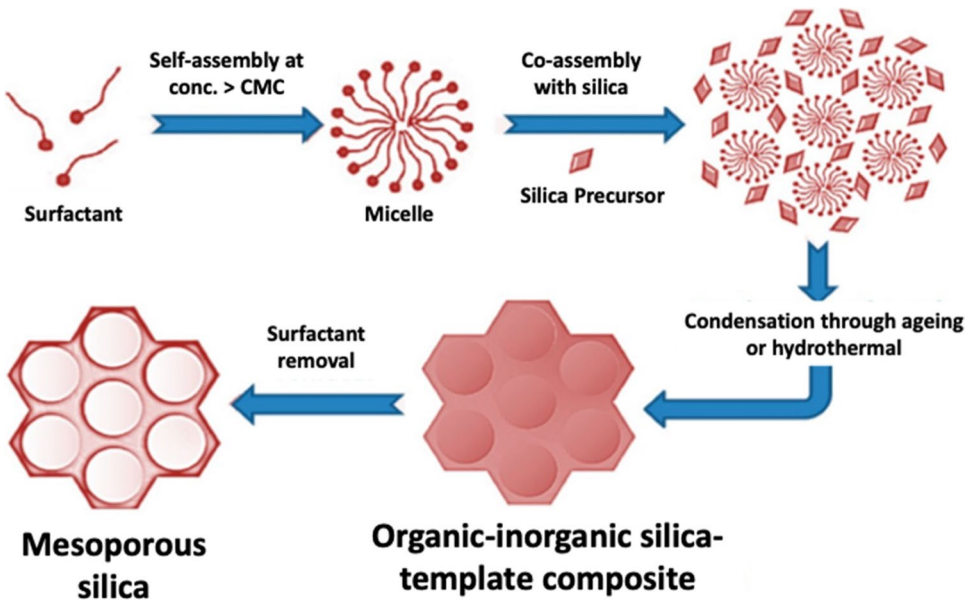

Fig. 3 Schematic diagram of mesoporous silica formation. [50]

3.6 Quenching Approach

As a result of the depopulation of the excited state of electrons within a molecule, it can be observed that quenching results in a molecular relationship between the fluorophore and the compound that quenches it, decreasing the fluorescence emission. It also refers to the act of slowing down or stopping a process before it reaches its final stage or cutting down on the components that go into a process or response [54]. Fowler et al. fabricated the MSN using the sol–gel quenching method. The response was retarded by adding too much water right after adding TEOS, as per the conventional MSN manufacturing protocol. The hydrolysis of TEOS was stopped after post-quenching for 60 secs by diminishing the reaction's fundamental characteristics by adjusting the pH of the reaction fluid. The description showed that the prepared MSN possessed a less structured framework and that a bigger particle-size MSN could be produced by postponing the neutralizing stage [55].

3.7 Flash Nanoprecipitation

The rapid mixing of two opposing streams carrying a mixture of dissolved materials and a stabilizing molecule that will precipitate is known as flash nanoprecipitation (FNP). The other has a solvent material that won't dissolve the stabilizer and dissolved solutes. Rapid mixing causes supersaturation and precipitation as well as turbulence [56]. By presenting successions in FNP, Fu et al. modified the sequence, giving it the moniker FNP. This modification aimed to create tetrads of tubes filled with a vortex mixture and joined to syringes. Two multi-inlet vortex mixers were coupled together by following these processes (each with dual tubing). The final two syringes, or the fourth syringe, had abamectin as the model drug, clean water in one, and Cetyl Trimethyl Ammonium Bromide (CTAB) solution in the other. High drug loading could also be achieved without needing a separate drug-loading period [57].

3.8 Sonochemical Approach

Methodologies for synthesizing nanomaterials have been designed with ultrasound irradiation, especially in aqueous media [58]. Passive bubbles form when a fluid is subjected to ultrasound waves. As a result of their final collapse (acoustic cavitation), these bubbles produce high pressure and temperature, which facilitate several chemical and physical processes (sonochemical processes), including covalent bond breaking, homogenization, and the formation of new molecules. Sonicated precursor mixtures comprising TEOS, base catalyst, and surfactant for 5 to 50 min at 43 kHz and 200 W of power [59]. Sonochemical synthesis, which utilizes one pot synthesis at room temperature to produce less agglomerated MSN has a large specific surface area and has a consistently spherical shape in the sub-micron range and is a straightforward commercial approach for making MSN on a large scale [59].

3.9 Biogenic Synthesis

For the purpose of getting rid of any undesirable pollutants, the husk is first cooked in an aqueous acidic solution. After that, it undergoes washing and is left to evaporate for an extended period of time. MSN is manufactured here using biological silica sources, predominantly rice and wheat husk, which is a resource that can be produced again, as the name implies [60]. The amorphous silica nanoparticles (SNPs) generated by the calcination of this dehydrated husk quickly melt in sodium hydroxide mixture to produce sodium silicate solution, which acts as a precursor silica source. This, under practical situations of usage, when added to a surfactant-rich solution, induces the precipitation of NPs; nevertheless, when the template is withdrawn, uniformly sized MSN are produced [61]. Because this method uses agricultural waste, it is inexpensive, secure, biocompatible, and advantageous to the surroundings, suggesting that a biogenic technique could be applied to the commercial manufacturing of MSN [62].

4 Factors Affecting MSN Synthesis

The parameters that affect the manufacturing process of MSN comprise silica precursor, reaction temperature, fluid pH, surfactant class and quantity, stirring speed, and duration [63]. The structure, size of particles, and pore diameter of the MSN are all going to be subject to changes in these characteristics, either directly or indirectly [64, 65].

4.1 Surfactants

MSNs are synthesized using surfactants [66–68]. The need for surfactant molecule aggregation during the synthesis of mesoporous materials is crucial because micelles must form later and serve as a template for creating pores and other structures [69]. The surfactant micelles, which are made up of anionic, nonionic, or cationic species that interact with the silica source through electrostatic force or hydrogen bonds, produce pores at the micellar interface. These interactions result in creating a mesoporous silica matrix [65, 66, 70]. A swelling agent can be used to make larger pores. It also can be applied to create mesoporous materials with clearly defined pores, and the kind and quality of the surfactant can be altered [71]. Surfactants utilized could be divided into the following categories:

i. Cationic surfactants have a nonpolar group and a positively charged polar hydrophilic head and hydrophobic tail. Hexadecyltrimethylammonium (HDTMA), cetyltrimethylammonium chloride (CTAC), and CTAB are among the alkali hydrophilic methyl ammoniums that make up the majority of these surfactants (CTAB) [72].
ii. Anionic surfactants. The surfactants' long hydrocarbon tail and negatively charged hydrophilic head have distinctive features [73].
iii. Ion-free surfactants. These are neutral surfactants, such as amide and phenol, with non-dissociable hydrophilic heads that are unable to undergo ionization in a water-based solution. Other instances are Triton X-100, polysorbate, Pluronic F127, and Pluronic P123 [73].
iv. Amphoteric surfactants, also known as zwitterionic surfactants, are unique because their hydrophilic ends contain positive and negative charges, which balance each other to produce a zero net charge. This makes them versatile in various applications, including personal care products, detergents, and industrial cleaners [6].

4.2 Co-surfactants

Co-surfactants, majorly alcohols such as ethanol [74] and butanol [75], which affect pore size, flexibility, and characteristics, constitute the vast majority of co-surfactant levels as they develop. When co-surfactant concentration increases, MSNs often misplace their round forms and form amorphous particles with chaotic pore sizes [76, 77]. Their capability of regulating the shape and pore size of MSNs increases their ability to transport medicines [6].

4.3 Solvents

Additionally, surfactants have a vital role in the manufacturing of MSNs. Ethanol, propanol, butanol, and pentanol are some of the toughest and most often employed alcohols. Alcohols influence mesopore size and promote pore development. Alcohols with downward evaporation speeds and heightened molecular weights, on the other hand, do not dramatically alter the morphology and form of mesoporous materials [6]. Alcohols also change the rotations of channels in mesoporous materials [78]. After the creation of MSNs, alcohols also aid in eliminating surfactants. To encourage the development of cylinder-shaped pores, alcohol has been employed as a solvent when creating circumferential MCM-48 [78]. The formation of aggregates of the generated mesopores could be prevented by using solvents to remove surfactants from those with high boiling points [79]. To make the silica precursor more soluble and hasten the hydrolysis process, alcohol can also be used in the reaction as a cosolvent [80].

4.4 Silica Sources

The production of well-ordered MSNs required an assortment of predecessors, including colloidal solutions of organosilanes, which include TMOS, TEOS, TPOS, and TMS, as well as sodium silicates [75]. The TMS predecessor exhibits a higher rate of silicate mesoporous development than alternative predecessors. The hydrolysis rate diminishes when the alkoxy groups' dimensions in silane mode increase because of a steric hindrance (spatial effects), particularly in heavily divided silica sources [81].

4.5 Temperature

The use temperature is essential in dictating the final characteristics of MSNs because mesoporous materials can be generated at temperatures ranging from 10 to 130° Celsius, with 25°C being the most suited [6]. Two important temperature-related variables must be considered: the critical particle temperature and the cloud point temperature (CP) (CMT). The CMT of surfactants must be under the synthesis temperature [81]. Increasing temperature can cause large particle sizes [82].

4.6 pH

MSN structures can be generated under either alkaline or acidic circumstances, as neutral circumstances fail to encourage the development of well-ordered constructions due to rapid polymerization and transverse bonding either synthesized under acidic or alkaline occurrences since neutral circumstances do not facilitate the synthesis of nicely ordered mesoporous structures because of high polymerization rates and transverse bonding [83]. However, well-ordered mesoporous materials can be produced under neutral conditions by altering the hydrolysis and condensation of the silica predecessors and using fluorine as catalysts [84]. pH changes during synthesis occur in an alkaline environment. Silica hydrolyzes at the start of the process, the pH decreases, the temperature rises slightly the silica species condense [65]. When the pH is reduced in highly acidic circumstances, the rate of mesoporous silica synthesis rises, and silica precipitation quantities increase when acid catalyst levels are sufficient [6].

4.7 Surfactant Removal After Synthesis

Surfactants can be removed after the formation of mesoporous silica structures using the following methods:

4.7.1 Calcination

The calcination process involves heating the created MSNs to high temperatures (800 °C) to fragment the surfactant.

The process consists in turning inorganic materials into hollow cylinders [85]. This method has limitations, including surface alteration, high temperature, and power needs. The surfaces and pores of the synthetic MSN material undergo compression due to the Si–OH bonds on its surface converting into Si–O-Si bonds at high temperatures. Consequently, the particle changes its pore size and becomes hydrophobic [68]. Furthermore, calcination generates the particles to become dehydrated and cross-linked, which causes irreversible aggregation of the particles and makes it challenging for the particles to separate back into single particles [86, 87].

4.7.2 Solvent Extraction

Solvent extraction is a milder solution to calcination that calls for intense thermal processing. Solvents that are acidic and/or alkaline can be applied to separate the produced nanoparticles according to the kind of surfactants and the circumstances of the experiment: ammonium nitrate, water, ethanol, hydrochloric acids, and other alcohols [88]. The solvent applied in extraction has less effect on the porosity and constructions of fabricated mesoporous materials than calcination. In most instances, solvent extraction does not remove all surfactants altogether, therefore recovered surfactants can still be used. This technique is excellent when total surfactant removal is unnecessary [89].

4.7.3 Chemical-assisted Oxidation

For the oxidation-based elimination of surfactants, hydrogen peroxide is a prominent chemical oxidizer [90]. This technique leads to a dropped volume of pore and surface areas despite increasing pore diameters [91]. Additionally, compared with calcinated samples, it boosts the amount of silanol groups on the silica sidewalls [92]. Hydrogen peroxide and an acid, like HNO3, frequently remove surfactants [91]. Other chemical oxidants used include ozone [93], Potassium permanganate, peroxides¸ and Ammonium perchlorate [94, 95].

4.7.4 Microwave Digestion

The most efficient technique for removing surfactant from mesopores is microwave digestion. It includes floating the generated mesoporous materials in a nNitric acid and a Hydrogen peroxide solution [96] or hexane and ethanol [97] solution before subjecting them to microwave radiation for approximately two minutes. Synthesized mesoporous materials' textural features are unaffected by this technique. Compared to calcined samples, it generates increased pore volume, size, and more extensive surfaces that enhance the number of silanol groups [98].

4.8 Effect of Synthesis Factors on the Physical and Chemical Characteristics of Mesoporous Silica

Following is a discussion of how synthesis parameters affect the physicochemical characteristics of materials made of mesoporous silica:

4.8.1 Pore Size and Shape

The dimensions and form of the mesopores control the types and quantities of drug molecules that may be retained by MSNs as well as the pace at which pharmaceuticals breakdown [99]. To prevent the rapid dissolution of medication molecules, the correct quantity of pore space must be used [100, 101]. The final pore size may depend on the kind, length of the chemical chain, and the surfactant concentration that can be used as templates [102]. The category chain length might impact the dimensions of pores and the quantity of surfactants employed as templates. Tetraalkylammonium salts, which are frequently utilized as surfactants, have been investigated by Jana et al. [103] for their impact on the pore sizes of MSNs. The pore size increased from 1.6 to 4.2 nm with a surfactant chain length from C8 to C22. Relevant investigations have also demonstrated that by varying the surfactant chain length, the size of the pores can be boosted to 4.1 nm [104, 105]. The selection of silica precursor, reaction duration, temperatures, and amount of catalyst are all essential variables for calculating the diameter of the pores of MSNs. Mesoporous materials with either 2D pores or 3D linked structures have different drug loads and release times depending on the hole sizes [106].

Additionally, as mesopore widths regulate the dimension of drug molecules stored inside the matrix, using the appropriate matrix is essential for optimal drug loading [107]. Drug molecules more minor than the cavity diameters are engrossed on the internal surface of the mesopore. On the other hand, inside the mesopore, molecules more significant than the cavities' diameters are absorbed on their surface. As a result, the size of the pores influences size-selective adsorption [108]. While this is happening, drug loading is considered an occurrence of the surface, and the entire surface area is significantly affected [109]. The combined amount of both outer is referred to as the total surface area. Surface functionalization and surfactant selection, type, and concentration can change it. Mesoporous materials are distinguished by their pore spaces, which display a total volume of pores that varies between 1–2 cm^3 g and an overall area of approximately 1000 m^2 g. The specific surface area of the matrices governs the number of drug molecules retained within matrices. [109, 110]. To retain additional medication molecules with a slower release rate, the surface area must increase because this creates more space for host–guest

interactions. The presence of Alendronate has been detected in matrix structures of SBA-15 and MCM-41. The kinetics of zero order was observed in the release of alendronate from SBA-15 (719 m^2 g) compared to alendronate use released from MCM-41 (1157 m^2 g) [111].

4.8.2 Particle Morphology and Surface Charge

The particles' size, shape, and surface charge significantly influence the drug transport capabilities of mesoporous materials. MSNs having a diameter of less than 1 nm exhibit quick mass transfer and better dispensability when compared to their bulk equivalents, making them highly sought-after for drug administration [68, 112, 113]. These molecules' surface charge and topology influence the pharmacokinetics of MSNs and their accumulation at target regions [114]. The internalization by mesoporous silicon nanoparticles (MSNs) cells, their cellular conversations, distribution in the body, and clearance are modulated by the size of the nanocarriers [115]. The surface charges of mesoporous materials also impact cellular absorption and in-vivo immune system reaction [114, 116].

The particle size of MSNs can be influenced by many variables, including pH, reaction temperature, stirring rates, types of silica precursors, and the addition of functional organosilanes, TEA as a base substitute, co-surfactants, and gelatin [102]. Moreover, it was observed that a rise in pH led to an augmentation in the hydrolysis rate of TEOS in conjunction with a larger particle size. Similarly, an elevation in the hydrolysis rates and polymerization of silica precursors with increasing reaction temperature led to the formation of MSNs with more excellent particle dimensions [68, 112, 117–119].

Various forms of MSNs can be produced by modifying reaction parameters such as the synthesis temperature, co-surfactant type, stirring rate, addition rate, and molar concentrations of water, silica source, surfactant, and catalyst [33, 99, 120]. The particle morphology of MSNs is influenced by slight fluctuations in the composition of reaction mixtures and their pH levels, as has been noted through empirical observation [121]. Cai et al. (171) generated shapes like spherical and silica rods through molar concentration modification of CTAB, TEOS, and $NaOH/NH_4OH$. The reduction of the condensation rate of silica was achieved by lowering the pH of the reaction mixture. This led to a decrease in the local curvature energy, ultimately forming SNs with discoid and spherical shapes [96].

5 Functionalization Techniques for MSN Drug Delivery Targeting and Regulation

The physicochemical properties of MSN constitute promising nanoplatforms for drug delivery. These properties include a high drug loading capacity, a large surface area, adjustable pore size and volume, good chemical stability, and biocompatibility. Furthermore, the functionalization of MSN is facilitated by the copious presence of free silanol groups on its surface. The use of MSN on the nanoporous material's inner and outer surfaces is encouraged by silanol groups. This feature offers several benefits, such as the regulated and prolonged delivery of bioactive substances, heightened efficacy towards the intended target, improved biocompatibility, and more significant conservation of biological materials [122]. The functionalization process does not affect the size or quantity of obtainable pores. However, when the internal permeability structures are functionalized, it enables the control and fine-tuning of host–guest chemistry, which is essential for the loading of drugs (Fig. 4) [123]. Contemplate functionalizing the internal pore structure to regulate and optimize the host–guest chemistry is essential for drug loading [124]. The pore's size and accessible space are not affected. A reaction mixture, including a template former and a silica source, is initially added before the available co-condensing reagent, such as organo-alkoxysilane, is added via a co-condensation technique. This method evenly covers the particulate's surface with the accessible substance. Since organic functional groups are introduced beforehand, they become a part of the particle and cannot be preserved by calcination as a template removal method [43]. Calcination can occur before or after the functionalization phase, whereas functionalization is performed after the NP is introduced (post-grafting) [125].

5.1 Targeted Delivery by MSN

Targeting is using a nanocarrier to administer a medicine or diagnostic to sick tissues only while minimizing the development of the nanocarrier in healthy tissues or cells. Passive targeting is made possible by the improved permeation and retention effect, where NPs preferentially accumulate at the tumor location since there is a leaky and loose blood vessel network. Active targeting is accomplished by lengthening the nanocarriers' circulation period while avoiding immune system surveillance. PEGylation exacerbated cytotoxicity due to improved cell penetration and sustained CUR release from PEGylated MSN, which stopped cell proliferation at all stages [127]. It's interesting to hear about the various approaches researchers have taken to enhance the efficacy and safety of MSNs in drug delivery applications. One approach is PEGylation, which involves coating the MSNs with polyethylene glycol (PEG) to increase their circulation time in the body and reduce the risk of adverse effects such as hemolysis [127]. In the case of puerarin-loaded MSNs, PEGylation enhanced the compound's bioavailability and reduced hemolysis [128].

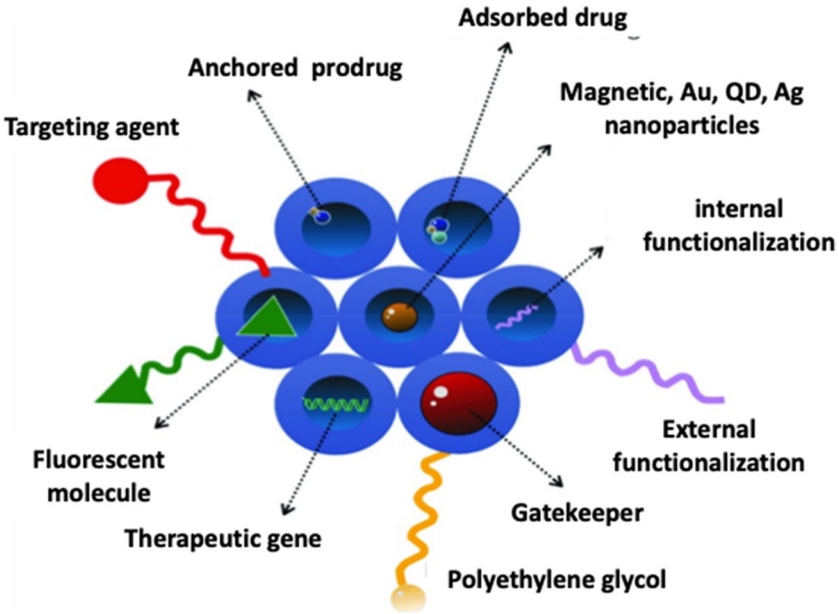

Fig. 4 Schemiaric skitch for surface functionalized MSN and its pores with variuos surface change. [126]

Another approach is lipid bilayer coating, which involves coating the MSNs with lipids to improve their biocompatibility and enhance their drug-delivery capabilities. In the case of ML336-loaded MSNs, lipid bilayer coating was found to suppress the Venezuelan equine encephalitis virus both in-vitro and in-vivo [129]. PEGylation has potential drawbacks, including rapid clearance, unexpected immunological responses, and decreased cellular absorption in tumorous tissues [130]. A targeting moiety (such as a ligand, antibody, protein, or peptide) is attached to the nanocarrier to target tissues with changed biochemical microenvironments. The cellular targets that the bound ligands engage with result in receptor-mediated endocytosis, which boosts DDS's therapeutic effectiveness by increasing cellular absorption. It is possible to bind ligands through chemical conjugation or physical adsorption [68].

5.2 Controlled Drug Delivery

The unexpected absorption of pharmaceuticals by normal cells and early drug dispersion from pore spaces throughout circulation throughout the body impede the effective implementation of the nano-system in therapies [131]. These problems make the nano-system challenging to utilize in treatments, even when tailored administration through ligand-mediated drug delivery to a particular organ, tissue, or cell is feasible. Stimuli-responsive caps (gatekeepers) may lock up the pores of MSN when precise therapeutic dose control is necessary, reducing leakage and payload degradation, lowering side effects and toxicity, and increasing the therapeutic impact of the drug [132]. Once the holes are sealed, the payload is delivered through polymers, host–guest assemblies, inorganic NPs, biomacromolecules, and other gatekeepers. Such internal or external stimuli as pH, redox, enzyme, temperature, magnetism, and UV radiation may activate these gatekeepers. Targeting sick tissue selectively is made possible by functionalizing ligands on the surface silanol groups, and stimuli-responsive gatekeeping allows the loaded medicine to enter the target tissue [133].

6 The Various Techniques for Regulating Drug Release Through Stimuli-Responsive Gatekeeping

The term "smart" refers to biomaterials that may change their characteristics in response to one or more inputs. The biomaterials' reaction to one or more stimuli may be reversible and take anywhere from minutes and hours. The stimuli could potentially be categorized in this way as physical, chemical, or biological (Fig. 5) [134].

6.1 pH-responsive

Drugs are only released when the intended pH is attained thanks to a pH-sensitive coupling between the sealing agent and nanocarrier. This hypothesis has been applied for generating MSN, which was incorporated with methotrexate and functionalized using chitosan (CHS) and 3-tri-ethoxy silyl propylamine [135]. The evidence indicates that the CHS coating exhibited a reduction in the viability of cancerous breast cells, even when exposed to low doses. Additionally, the coating enhanced and improved the cellular uptake of drug-loaded MSN. Resiquimod (R848), an immunostimulant, was incorporated into the pores of MSN. Subsequently, a pH-sensitive acetal linker featuring biotin-conjugated at

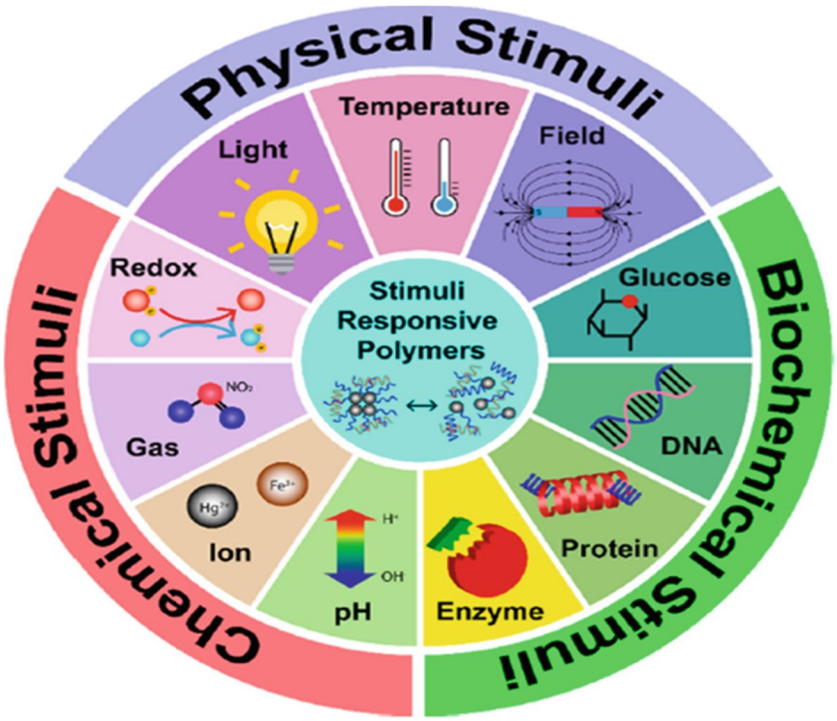

Fig. 5 Schematic illustration of the different stimuli-responsive polymer, *2021, American Chemical Society* [134]

the periphery was affixed onto the exterior of MSN. The avidin and the biotin interacted non-covalently to form the biotin-avidin mixture. Exposure of manufactured NPs to macrophage cell lines resulted in significant immune system responses, suggesting efficient intracellular payload transport [136]. Aminated MSNPs (AMPSNPs) were synthesized as pH-responsive disulfiram-delivery [137].

6.2 Redox-responsive

Glutathione (GSH) is the principal scavenger of reactive oxygen species (ROS) and nitrogen species and a tripeptide that is present in cell organelles [138]. It does this by preserving the balance of redox conditions within the cells. Glycine, glutamate, and cysteine are the amino acids that make up this substance. To scavenge excessively produced intracellular ROS and detoxify xenobiotics, malignant cells need increased GSH levels [139]. For this reason, GSH is used for targeting the release of nanoparticles [140–142]. To reduce the medication released into the tumor, MSN was co-loaded with paclitaxel and the P-glycoprotein inhibitor quercetin. The dialysis procedure at pH 7.4 with or without 20 mM GSH was used to study drug release. Likewise, 20% of the compound was released when no GSH was present, but over the course of 36 h, approximately 65% of the compound paclitaxel and 52% of the compound quercetin were released [143].

The release of drugs in response to redox was induced by the cleavage of the gatekeeper from the surface of NP through disulfide by GSH. No cytotoxicity was detected for empty MSN at concentrations up to 100 g/mL in-vitro. However, cancer cells exhibited significant internalization of DOX-MSN. An additional study by S. Zhao et al. [144] showed that the redox-responsive approach utilizing MSN as a core DDS had been found to be effective in delivering DOX and siRNA to tumor cells for targeted cancer therapy and drug release control. The results of this study suggest that the redox-responsive approach utilizing MSN as a primary drug delivery system (DDS) may be a viable means of effectively administering DOX and siRNA to tumor cells, thereby targeting cancer and regulating drug release [145].

MSNs nanoreservoirs collagen end-capped was fabricated results showed a remarkable ability for redox-responsive drug release as well as cell-specific targeting [146]. Another multifunctional MSN tagged with phenyl boronic acid and pore blocking with gold nanoparticles for targeted a redox-responsive controlled drug delivery into tumor tissue [147].

6.3 Enzyme-responsive

Enzymes are essential to many biological processes, and they are expressed in sick cells and tissues in varied ways. For instance, malignant and inflammatory tissues have elevated expression levels of phosphatases, proteases, and glycosides [148]. Therefore, enzyme-specific ligands could have adhered to medication-loaded NPs to target particular

sick tissues and improve the therapeutic efficacy of the medicine. Delivering specific medications to the colon via MSN Since no drug was released at any of those pH levels without colonic enzymes (derived independently from colonic microflora), Kumar et al. [149] prepared MSN. The researchers loaded the 5-fluorouracil (5-FU) anticancer agent and coated it with guar gum as an enzyme-responsive gatekeeper. This coating effectively inhibited cargo release from the pores, as demonstrated by the results of in-vitro release. However, 40% of the total loaded medication was destroyed by increased enzyme concentrations. According to published studies, the protease family member matrix metalloproteinase is overexpressed in tumor cells, and collagen is a favorable substrate for these enzymes. Based on the chemistry of the enzyme substrates, collagen was used to functionalize MSN that had been loaded with cisplatin [150].

6.4 Thermo-responsive

The phrase "thermo-responsive polymer" refers to materials whose physical characteristics sharply alter with temperature. Such polymers can display either a lower critical solution temperature (LCST) behavior or an upper critical solution temperature [151]. Over the LCST, the polymer either expands or shrinks due to its insolubility. Under the LCST, the polymer completely disintegrates in the solvents [152]. Accordingly, Ugazio et al. connected poly (NIPAM) to the pore walls of MSN, loaded it with quercetin, and then 3-methacryloxypropyl trimethoxysilane was copolymerized by free radicals. This method yields a different pore size of MSN (small and large). Rapid initial drug release was seen at both 20 and 40°C in the smaller one, while a 20% greater drug release at the latter temperature owing to the copolymer's thermal reactivity exhibited by the larger MSNs. The smaller MSNs showed more excellent drug trapping but less thermoresponsive drug release because the drug was mainly physisorbed to the outside of the NPs release [153].

6.5 Reactive Oxygen Species-responsive

The concept of oxidative stress was introduced by Helmut Sies and Dean Jones, who defined it as an imbalance between oxidants and antioxidants, with a bias towards the former. Under oxidative stress conditions, a significant amount of reactive oxygen species (ROS) can be observed, comprising singlet oxygen, hydrogen peroxide (H_2O_2), superoxide anion radicals, hydroxyl radicals, and hypochlorous acid/hypochlorite. Several ROS-responsive nanocarriers have been investigated to deliver medication to specific regions with elevated ROS levels. Helmut Sies and Dean Jones defined oxidative stress as the balance between oxidants and antioxidants that favors the oxidants [154]. As a means of delivering medication to target locations with high ROS concentrations, many ROS-responsive nanocarriers have been investigated. Further, Shen et al. [155] established resveratrol-loaded MSN with polylactic acid caps for brain targeting. Burst release 50% was seen after one day and 90% after five days in studies on in-vitro release in the presence of H2O2. To increase skin penetration and control the glabridin release pattern, Du et al. [156] synthesized amine-functionalized HMSN and end-linked it with 4-carboxyphenylboronic acid.

6.6 Magnetism-responsive

Using externally administered magnetic radiation on target organs and tissues, MNPs have been researched for targeted drug delivery and diagnostics. They are constructed by synthetic materials, including ferrous, nickel, cobalt, and a few rare earth metals, and are coated with biocompatible compounds to make them more biocompatible. The process of combining bioactive agents to surfaces facilitates targeting [157]. The method for delivering drugs via magnetism involves gatekeepers that respond to stimuli, magnetic field-guided drug targeting, and hyperthermia, a unique property of MNPs that could eradicate cancerous cells [158].

Further, Asgari et al. [159] created a mesoporous silica layer on iron oxide NPs. Radical polymerization was used to attach NIPAM copolymerized with acrylic acid to the surface of silica. Importantly, 5-FU drug release was monitored while the model drug was put into the pores. AMF-applied NPs showed a persistent discharge after an initial burst release (50% drug) over two hours. Besides, Peralta et al. [160] coupled thermosensitive copolymer poly [NIPAM-co-3-(methacryloxypropyl) trimethoxysilane] with core–shell iron oxide NPs coated with mesoporous silica layer and discovered comparable results. Only 20% of the total loaded medication was released from the copolymer-capped NPs when the temperature reached 25 °C (below LCST). As opposed to this, at 40 °C (above LCST), the copolymer undergoes a coil-to-globule transition, which opens the pores and causes the whole amount of loaded medicines to be released from the NP's apertures over the course of 24 h.

6.7 Ultrasound-responsive

Recent developments in the ultrasonics, ultrasound is widely used in the medical field for therapeutic as well as diagnostic purposes [161]. It produces the biological effects through three different mechanisms: mechanical (acoustic cavitation and bilayer sonophoretic action), thermal (hyperthermia-induced cell death), and chemical (generation of ROS) [162]. When X. Li et al. [163] researched ultrasound-induced acoustic cavitation, they attached the alginate strands onto the terminal amine chains and laminated the surface silanol chains of MSN.

6.8 Light-responsive

Targeted DDS uses light in one of three wavelength ranges, 650–900 nm the most popular used, near-infrared (NIR, 750–2000 nm), visible (400–750 nm), and ultraviolet (200–400 nm). A dye-peptide mixture, specifically the antimicrobial peptide PA-C1b (palmitic acid conjugated chanson-1 b), was introduced into MSN's pores [164, 165]. They filled the pores with FA-conjugated graphene oxide to treat cancer using infrared-induced drug release. After being exposed to NIR (808 nm) for 10 min, in-vitro release started exhibiting abrupt and photo-induced release behavior. In the absence of radiation exposure, NPs showed no release. In a different experiment, Ag NPs that had previously been encapsulated in the HMSN core by IBU-encapsulated HMSN pores had their photo-responsive switch made of NIPAM copolymerized with acrylic acid. About 50% of the release was observed [166].

6.9 Adenosine Rriphosphate (ATP)-responsive

ATP concentration has been optimally regulated by nature in various organs and organelles. However, malignant and ill cells exhibit opposite variations in ATP concentration. At the specified site, two distinct, separate strands of DNA had previously been affixed to the surface of MSN, with an aptamer sensitive to ATP being intercalated between them. The aptamer undergoes cleavage in response to an ATP attack, exposing two separate strands of DNA and thus generating an opening to release the encasing chemical. ATP sensitivity was the highest when comparing the aptamer to different nucleoside triphosphates. This theoretical protest might therefore be applied in ATP-responsive MSN for drug delivery [167–169].

6.10 Hypoxia-responsive

The microenvironment surrounding a tumor is characterized by a lack of oxygen which exhibits an arrangement of expression that includes particular molecules and enzymes like nitro reductase and decreased phosphate, supplying the possibility to develop hypoxia-responsive DDS. For instance, incorporating an azobenzene derivative in a nanocarrier structure has proven the breakdown of azo bonds, resulting in controlled drug delivery in a dehydrated state condition [170]. Similar to nitroimidazole, which experiences fragmentation and decreases in hypoxic environments, nitroimidazole is being investigated extensively as a treatment for hypoxia. In order to control the release of DOX, nitroimidazole was end-linked to MSN's surface and coupled with a-CD to produce a hypoxia-sensitive gatekeeper. The delivery of medications to cancer or any other disease that illustrates hypoxia may be targeted using these hypoxia-responsive NPs [68].

6.11 Electro-responsive

MSNs grafted with electro-responsive polymers as a method for controlling the biomolecules release has been recently investigated. [171–173]

N-3-Triethoxysilyl propyl ferrocene carboxamide onto the surface of rhodamine 6G-loaded MSN, locking an electro-responsive gate over the pores. However, the oxidation peaks detected by cyclic voltammetry demonstrate that the electrooxidation of the ferrocene moiety and the external application of voltage shifted the polymer's nature toward hydrophilia, despite the absence of peaks of only MSN. Only 4.41% of the payload leaked while no electrical current was supplied, but after 24 h slow, and gradual voltage-dependent leakage of around 48.19% was observed [174].

6.12 Glucose-responsive

Utilizing the blood glucose level as stimulus Hou et al. developed MSN decorated with carboxyphenylboronic acid coated by sodium alginate to form boronate ester insulin loaded. In-vitro studies have demonstrated that the release of insulin occurs promptly upon establishing a hypoglycemia environment, contingent upon the level of GLU present in the medium [175]. Likewise, Huang et al. [176]conducted comparative research to control insulin release during hyperglycemia. Here, MSN was coupled with 3-fluoro-4-carboxyphenylboronic acid, and insulin was then injected into the pores. Following this, the coupler was connected to the copolymer poly (NIPAM-co–N-acryloyl glucosamine) by an ester link, producing a borate ester just like in the earlier research. The cumulative release experiment demonstrated a progressive increase in insulin release over time, demonstrating the functionalized MSN's increased GLU sensitivity. This resulted from the copolymer coat rupturing because the GLU was able to bind successfully to the borate link.

6.13 Miscellaneous

According to the phenotype, the neuroendocrine carcinoma identified as pheochromocytoma discharges noradrenaline, dopamine (DOP) and adrenaline. By grafting azide-functionalized DOX-MSN with alkyne-modified DNA, which served as a template for Ag NPs, Yang et al. [177] created a DOP-responsive nano-platform to target DOP-secreting pheochromocytoma. Since the mineral biotin (vitamin-H) can be detected in more significant quantities in cancerous tissue, the MSN-based NPs were developed by Le Li et al., who first desthiobiotin-linked the amine-functionalized MSN-based NPs on the surface [178].

7 Dual Stimuli-responsive Drug Delivery

Focusing on a particular stimulus may lead to premature or indiscriminate drug release. Thus, a more suitable approach for accurate payload management would be through dual or double stimuli-responsive controlled release. Nonetheless, this methodology exhibits a limitation in that it necessitates the presence of both stimuli at the intended release location to activate the release of drugs independently [179]. Additionally, compared to healthy tissue, malignant tissue has a variety of constituents or variables with changed amounts, such as an acidic pH, hypoxia, higher levels of ROS, GSH, GLU, ATP, etc. [180]. For example, Folic acid, HER2/neu antibodies, as targeting ligands for cancer cells, were attached to the MSNPs [181].

Human hair keratin, a biocompatible, biodegradable protein that exhibits pH and GSH responsiveness, for cancer-targeting needs. The protein underwent complexation on the surface of polydopamine (poly-DOP) layered doxorubicin-loaded (DOX-MSN) through the formation of iron (III)-mediated coordinate bonds. Upon exposure to NPs generated with DOX at a concentration of 10 g/mL, the viability of L929 cells, which are healthy, was observed to be approximately 1.5 times higher than that of A549 cells, which are malignant. The study followed an enhanced release of drugs in cancerous surroundings, as demonstrated by a gradual increase in DOX fluorescence within malignant cells, indicating an ongoing release feature. [182]. Yumei Wang et al. glued phenylboronic acid pinacol ester over the MSNR surface and trapped DOX in the pores (decorated DOX-MSNR) to integrate pH and ROS dual-responsive releasing nature to MSNR. After that, a CD-modified hyaluronic acid conjugate was connected to the boronic ester via supramolecular contact. This attachment broke when the pH dropped, and the medication was released most effectively at pH 5, followed by pH 6.5 and 7.4. After this cleavage, DOX release was enhanced when boronic ester was exposed to the outside environment (where artificial H_2O_2 was introduced) [183].

8 Triple Stimuli-responsive Drug Delivery

Taking one step further, tri/triple stimuli-responsive MSN is being constructed and examined for improved healthcare delivery. The altered MMSN with the addition of a thiol group in a single pot, attached to S-(2-aminoethylthio)-2-thiopyridine hydrochloride using a disulfide linkage, and then coated the exterior with poly (NIPAM). DOX putting was performed at 50 ℃ (above LCST) in dark conditions where globule to coil conversion of poly (NIPAM) led to drug completing into the pore spaces, thus provided an earlier purpose that drug release would take place above LCST, which surfaced to be genuine when investigated for in-vitro drug release, where 10% of DOX released at 25 ℃ (below LCST) anyway around 50% release occurred at 40 ℃ (above LCST) within 10 h. When 10 mM tris (2- carboxyethyl) phosphine was utilized as a reductant to enhance the hydrodynamic diameter of NPs from 255 to 458 nm in 2 h, disulfide bond breakage was verified. When a reducing agent was added to the mixture, the drug's release via the synergistic interaction of temperature and reducing agent was confirmed, showing, respectively, 65% and 80% cumulative release at 25 °C and 40 °C within 24 h. At 25 °C without a reductant, by comparison, fewer than 20% of the medicines were released. Magnetism-stimulated drug release is brought on by magnetic hyperthermia, which transforms poly (NIPAM) from globule to coil. To create pH, redox, and light-responsive MSN for battling cancer, DOX-MSN was treated with the photosensitizer hematoporphyrin. Then, individually cesium oxide NPs were placed over the surface in a one-pot procedure. The drug release process included converting cerium oxide NPs to cerium ions under the influence of GSH and a lowered pH.

In contrast, the cerium oxide NPs were destroyed by UV light. Another study produced and loaded tiopronin into the pores of a mesoporous silica shell using similar combinations of stimuli. The copper sulfide nanosphere functioned as the core for the disulfide link doped MSN. CUR (as a fluorescent chemotherapeutic agent) and CHS formed a Schiff base connect, capping CHS to serve as an unpleasant release blocker and end-linking it to CUR [184].

The overall percentage of release increased to 63.30% with an increase in GSH concentration from 5 to 10 mM, demonstrating that GSH concentration affects release. Applying NIR light increased the total release in both pH 5.0 and pH 7.4, indicating light-responsive release (caused by the photothermal conversion of the core), and the maximum cumulative release from NIR irradiation NPs reached 91.90% in pH 5.0 with 10 mM GSH, within 48 h. This CUR-decorated core–shell MSN loaded with tiopronin can be used for imaging purposes in addition to chemotherapeutic delivery, specifically to tumors [185].The fluorescent magnitude from CUR reduced considerably from 4 to 48 h in acidic (pH 5.0) [186].

9 Regulated Release Through a Hybrid Nanocarrier

It takes a complicated one-piece dual nanocarrier system consisting of MSN and another nanocarrier to transport many drugs and focus on a specific area for controlling release in response to stimuli.

9.1 MSN-liposome

In the past, MSN and liposomes have been coupled by coating the MSN with a double layer of lipids over the peripheral surface to enhance stability, boost drug loading efficiency, sustain payload release, and avoid early using a lipid bilayer structure that is pH sensitive [185]. The study compared the pH-responsive release of a nanocomposite and another nanocomposite, wherein pH-sensitive nanoparticles exhibited the release of over 80% DOX, while pH-non-sensitive nanoparticles released only approximately 60% DOX over a period of 36 h. The present study reports the development of a nanocomposite comprising a pH-insensitive bilayer of lipids and DOX-MSN. The nanocomposite possesses a dual drug delivery capability owing to the flexibility of the lipidic bilayer, which enables it to accommodate any hydrophobic drug while also remaining unoccupied. Feng et al. [187] investigated this dual drug delivery strategy and a stimuli-mediated release mechanism.

9.2 MSN-dendrimer

A class of organic nanocarriers with a three-dimensional morphology is called dendrimers. They serve as medication delivery systems to increase effectiveness and lessen toxicity. X. Chen and Liu [188] successfully completed a project to create anticancer nanocomplexes based on dual stimuli-sensitive releasability. MSN that has been functionalized with 3-mercaptopropyltrimethoxysilane was disulfide-linked to 2-(pyridyldisulfanyl) ethylamine. The terminal amine was connected to fluorescein isothiocyanate (a dye), and methotrexate was injected into the pores. A second-generation polyamidoamine-based dendrimer compound was joined with the dye as a nanocarrier cap to load DOX and clog the pores. Hyaluronic acid produced a shell over the nanocomposite by electrostatic interaction. Dendrimer (-CD) for stimuli-mediated dual drug delivery was made by mixing MSN and -CD-enhanced polyamidoamines. Redox-responsive disulfide-linked azido linkers joined the interior walls of the holes, whereas the surface amine groups were bonded by ROS-responsive nitrophenyl benzyl carbonate. Anticancer medication SN-38 and therapeutic gene Bcl-2 siRNA was added to the MSN's apertures after capture [dendrimer (-CD)]. Extruding the nanocomposite from the 4T1 cancer cell's membrane led to successful NPs. After 40 and 20 h, accordingly, the GSH-triggered leakage showed > 82% (SN-38) and > 60% (siRNA) release. Using membrane-coated NPs, in-vitro cytotoxicity on 4T1 cancer cells had the most significant influence on cell death [189].

9.3 MSN-nanofiber

Drug-filled MSN has been combined in the nanofiber structure to ensure the continued release of drugs. For this explanation, rather than being laden in MSN, the NPs are inserted in either dosage-less nanofiber (mono drug delivery) or distinct drug-laden nanofiber (dual drug delivery). Moreover, comparable medicines have been incorporated into NPs and nanofibers implementing MSN-nanofiber composites (mono-drug delivery), which led to delayed, sustained drug release over a longer time frame [190]. To produce scaffolds for bone regeneration, dexamethasone-loaded MSN was coated with CHS, and these NPs were then dispersed in a poly-lactic acid solution and electrospun. Due to this, the MSN-nanofiber composite exhibited stimulus-responsive activity [184]. Additionally, Samadzadeh et al. created an MSN-nanofiber composite that responds to magnetism. Using LCST 48 ℃, a temperature-sensitive copolymer solution of poly (NIPAM-co–N-hydroxymethyl acrylamide) was used to disperse iron oxide MNP and metformin-encapsulated MSN. The necessary AMF-sensitive scaffold was created by electrospinning this solution [191].

9.4 MSN-MSN

A hybrid nanocarrier platform can be created by combining two MSNs, amplifying the benefits of each MSN and improving medication delivery methods. Through supramolecular co-assembly of two heterogenous MSNs, one of which contained a sizable pore filled with melittin and functionalized with -CD-modified polyethyleneimine chains, a dual drug carrier scaffold comprising both ofloxacin (OFL) and melittin (MEL) was produced [192].

10 Biomedical Applications of MSNs

MSNs are employed in several medicinal, biological, and imaging applications (Fig. 6). While bioimaging might improve organ visibility, therapeutic applications can increase the bioavailability of medications with active ingredients. MSNs contain a medicine that is loaded to have the desired effect. Delivered medications include anti-inflammatory and anti-cancer medications, and other active ingredients that boost the body's immunological responses have also been loaded. Additionally, due to their high drug loading and entrapment effectiveness, MSNs are appropriate for encasing a variety of medicines, increasing the efficacy of the formulation [15].

11 MSNs in Cancer Therapy

Mesoporous silica nanoparticles have shown great potential in cancer treatment due to their unique properties, such as high drug loading capacity, controlled drug release, and surface functionalization for targeted delivery. MSNs have great potential in cancer treatment, and ongoing research

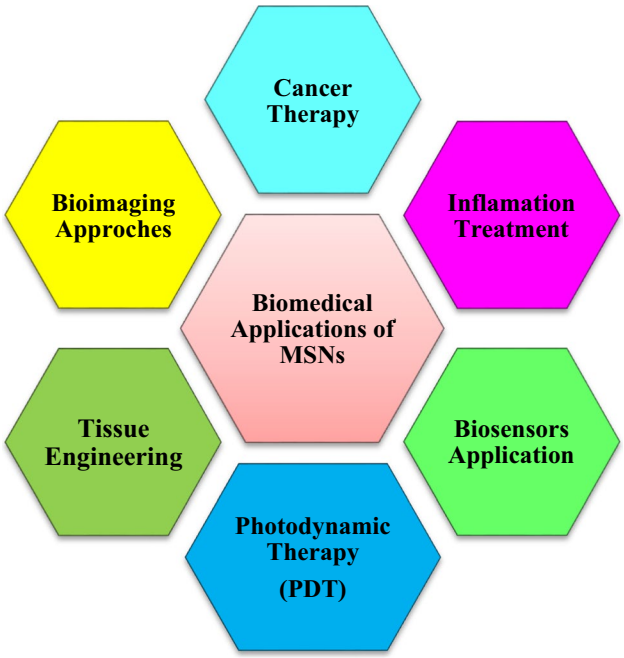

Fig. 6 Feasible application of MSN in various medical and pharmaceutical fields

is exploring new ways to utilize their unique properties to improve cancer therapy and patient outcomes [137]. Two mechanisms are involved in creating multifunctional MSNs responding to targeted activated stimuli. The first step is the creation of MSNs with active target ligands that serve as capping agents on their surface. By making this alteration, drug targeting, and controlled release goals at the desired region are perpetrated. PEGylated MSNs that are nucleolin-targeted have been successfully used to treat colorectal cancer. Rod-shaped MSNs were created and packed with camptothecin and shRNA, enabling simultaneous co-delivery to the desired location. Additionally, the aforementioned medication and RNA-loaded MSNs have been tagged with the AS1411 DNA aptamer for selective treatment against colorectal cancer. In animals with the C26 tumor, the medication and RNA-loaded MSNs displayed regulated release and may have inhibited tumor development. Therefore, the created MSNs can potentially be exploited as a delivery system for RNA and medication to treat colorectal cancer [193].

Though radiotherapy (RT) has successfully treated cancer, its therapeutic effects, metastasis, and recurrence remain significant obstacles. Li et al. [194] created hydroxychloroquine (HCQ) encapsulated hollow MSN for improved radiation treatment and autophagy suppression to increase radiosensitivity and overcome radio-resistance. These HMSNs significantly reduce the effectiveness of conventional radiation by acting as radiosensitizers. Recent reports additionally address using MSNs in photothermal treatment, radiation, and magnetic-responsive delivery of drugs. Cao et al. [195] developed pH-sensitive MSNs for photothermal medication to eradicate liver's cancer.

11.1 MSNs in Inflammation Treatment

Nonsteroidal anti-inflammatory drugs have also been delivered using MSNs for possible biological purposes. For instance, Celastrol-loaded MSNs were created by Jin et al. [196] to treat osteoarthritis. And to develop pH-dependent drug delivery systems, the MSNs have been coated with chitosan. MSNs with ibuprofen in them were created to alleviate musculoskeletal pain. According to Li et al., [197] silica nanoparticles coated in cotton textiles may transport NSAIDs, including ibuprofen, diclofenac, and salicylic acid. Therefore, it can be said that functionalized silica NPs have prospective uses in topical formulations that resemble creams and ointments for the development of anti-inflammatory agents.

11.2 MSNs in Bioimaging Approaches

MSNs can be used as imaging agents to visualize tumors and monitor their response to treatment. MSNs can be loaded with imaging agents such as fluorescent dyes or magnetic nanoparticles, allowing them to be detected using imaging techniques such as fluorescence imaging or magnetic resonance imaging (MRI). Chemical stability and a variety of physiological body circumstances are required for a substance to be utilized as a bioimaging agent. The formulation should have good contrast imaging capabilities, a long blood circulation duration, and be in colloidal in-vitro and in-vivo [198]. Dual-mode fluorescence probes were created because standard fluorescent probes might be weak. MSNs containing gadolinium ions and red AIE color Using MRI and fluorescence imaging, incorporating the ions and dye into the MSNs offers an excellent opportunity for formulation detection. This newly created MSN-based formulation helps to improve the present bioimaging techniques [199].

11.3 MSNs in Photodynamic Therapy (PDT)

PDT is a cancer treatment that involves the use of photosensitizers and light to generate reactive oxygen species (ROS) that can destroy cancer cells. MSNs can be loaded with photosensitizers and delivered to tumor cells, where they can be activated by light to induce cancer cell death. ROS is a fast-acting, cell-killing oxygen free radical excellent for treating malignancy. PDT may also be utilized to demonstrate antibacterial activity for infections of the ears and eyes. The light source turns the photosensitizer on, which also destroys unhealthy cells. The formulation may also be administered intravenously,

and following administration, the targeted organ may be exposed to light. One study used MSNs supplied with zinc-phthalocyanine, labeled with cetuximab antibody, and 131I radionuclide to identify the pancreas-targeting antibody [200].

11.4 MSNs in Biosensors Application

MSNs have shown great potential in biosensors due to their unique properties, such as high surface area, tunable pore size, and biocompatibility [201–203]. Chen et al. [204] created mesoporous silica nanoparticles coupled with a chemiluminescence (luminol/H2/O2) system to create the biosensor. The model drug was cocaine, and MSNs and glucose were administered. The positive charge of the MSNs containing glucose reacted with the negative electrical charge of the cocaine aptamer. In a different research investigation, Sandra et al. created avidin-gated MSNs for electrochemical biosensor applications. MSNs were loaded with the signal-boosting agent avidin/iminobiotin-functionalized methylene blue, a redox probe. Sulphuric acid incubation of the produced MSNs formulation permits the release of the encapsulated redox probe and facilitates the identification of cancer biomarkers [205].

11.5 MSNs in Tissue Engineering

Regenerative medicine, often known as tissue engineering, is a young science that seeks to improve or repair the function of injured tissues by creating scaffolds with potential therapeutic properties. The ideal tissue-engineering scaffold offers directed differentiation, robust cell adhesion, and growth behavior to develop novel tissues or organs. MSN-based scaffolds are built to boost prepared scaffolds' mechanical characteristics because of their potential stability and simple surface modification [206]. Satar et al. [207] prepared a chitosan/alginate nanocomposite conjugated with MSN for use in the field of bone engineering. MSNs were first produced and loaded with a composite scaffold made of alginate and chitosan that had been freeze-dried. MSNs were added to the constructed scaffold to increase mechanical strength, with little to no impact on porosity. The scaffold demonstrated a better capacity for biomineralization than the basic alginate/chitosan scaffold and was non-cytotoxic. It was discovered that the MSNs with the alginate/chitosan scaffold had guarantee uses in bone tissue engineering [207].

The Future prospective Mesoporous silica applications in the biological field can be optimized by Central composite design (CCD) via optimization study of response surface methodology (RSM). This technique improves experimental accuracy, reduces the number of experimental trials, and increases the amount of information available for measuring goodness of fit. Also, artificial intelligence (AI) and machine learning can be applied in tissue engineering by mesoporous silica. AI approaches have been used to predict the performance of drug molecules in mesoporous silica. Various AI algorithms such as artificial neural networks (ANN), genetic algorithms (GA), and adaptive neuro-fuzzy inference systems (ANFIS) have been applied to predict carrier efficacy.

12 Conclusion

A silica material known as mesoporous silica has a large surface area and a well-defined pore structure. Due to this, it is a material well-suited for biological applications, especially drug delivery systems. Surfactants serve as templates to regulate the pores' size and configuration during mesoporous silica synthesis. Other compounds, such as medication molecules or targeted ligands, may be functionalized to increase the material's selectivity and effectiveness. Transmission electron microscopy (TEM), X-ray diffraction (XRD), and nitrogen adsorption/desorption studies are often used to characterize mesoporous silica. These methods may provide details regarding the material's dimensions, internal organization, and surface characteristics, which are crucial for enhancing its efficacy in drug delivery applications. Several biological applications, such as medication administration, gene therapy, and imaging, have used mesoporous silica. It is large surface area and pore structure enable regulated drug release and high drug loading, which may increase the effectiveness and safety of pharmacological therapies. The material is also a good contender for various therapeutic applications due to its biocompatibility and low toxicity. Ultimately, creating innovative drug delivery systems and other biological applications is a significant field of study in synthesizing and characterizing mesoporous silica.

Author Contribution Mayssa Abdel Hady wrote the whole review and revised it.

Funding Open access funding provided by The Science, Technology & Innovation Funding Authority (STDF) in cooperation with The Egyptian Knowledge Bank (EKB).

Data Availability All data generated or analysed during this study are included in this manuscript.

Declarations

Ethics Approval Not applicable.

Consent to Participate Not applicable.

Consent for Publication Not applicable.

Competing Interests I declare no competing interests.

References

1. Wang H et al (2011) Shape- and size-controlled synthesis in hard templates: sophisticated chemical reduction for mesoporous monocrystalline platinum nanoparticles. J Am Chem Soc 133:14526–14529
2. Xu Y, Jin S, Xu H, Nagai A, Jiang D (2013) Conjugated microporous polymers: design, synthesis and application. Chem Soc Rev 42:8012–8031
3. Sher P, Ingavle G, Ponrathnam S, Pawar AP (2007) Low density porous carrier based conceptual drug delivery system. Microporous Mesoporous Mater 102:290–298
4. Brownscombe TF, Bass RM, Corley LS (1993) Process for preparing low density porous crosslinked polymeric materials. https://patents.google.com/patent/EP0712425A1/en
5. Nagai K, Musgrave CSA, Nazarov W (2018) A review of low density porous materials used in laser plasma experiments. Phys Plasmas 25:030501
6. Mirzaei M et al (2020) Silica mesoporous structures: effective nanocarriers in drug delivery and nanocatalysts. Appl Sci 10:7533
7. Galzerano B et al (2018) Design of sustainable porous materials based on 3D-structured silica exoskeletons, Diatomite: Chemico-physical and functional properties. Mater Des 145:196–204
8. Wu T et al (2018) Relationships between shelter effects and optical porosity: A meta-analysis for tree windbreaks. Agric For Meteorol 259:75–81
9. Das S, Heasman P, Ben T, Qiu S (2017) Porous Organic Materials: Strategic Design and Structure-Function Correlation. Chem Rev 117:1515–1563
10. Sun MH et al (2016) Applications of hierarchically structured porous materials from energy storage and conversion, catalysis, photocatalysis, adsorption, separation, and sensing to biomedicine. Chem Soc Rev 45:3479–3563
11. Rouh H et al (2018) Synthesis of Functionalized Chromene and Chroman Derivatives via Cesium Carbonate Promoted Formal [4 + 2] Annulation of 2′-Hydroxychalcones with Allenoates. J Org Chem 83:15372–15379
12. He S, Sun G, Cheng X, Dai H, Chen X (2017) Nanoporous SiO2 grafted aramid fibers with low thermal conductivity. Compos Sci Technol 146:91–98
13. Li T, Geng T, Md A, Banerjee P, Wang B (2019) Novel scheme for rapid synthesis of hollow mesoporous silica nanoparticles (HMSNs) and their application as an efficient delivery carrier for oral bioavailability improvement of poorly water-soluble BCS type II drugs. Colloids Surf B Biointerfaces 176:185–193
14. Lu J, Liong M, Li Z, Zink JI, Tamanoi F (2010) Biocompatibility, biodistribution, and drug-delivery efficiency of mesoporous silica nanoparticles for cancer therapy in animals. Small 6:1794–1805
15. Vallet-Regí M (2022) Our contributions to applications of mesoporous silica nanoparticles. Acta Biomater 137:44–52
16. Michorczyk P, Ogonowski J, Niemczyk M (2010) Investigation of catalytic activity of CrSBA-1 materials obtained by direct method in the dehydrogenation of propane with CO2. Appl Catal A Gen 374:142–149
17 Srinivasu P, Vinu A (2008) Three-dimensional mesoporous gallosilicate with Pm3n symmetry and its unusual catalytic performances. Chem Eur J 14:3553–3561
18. Huo Q et al (1994) Generalized synthesis of periodic surfactant/inorganic composite materials. Nature 368(6469):317–321
19. Shi C et al (2015) Low temperature oxidative desulfurization with hierarchically mesoporous titaniumsilicate Ti-SBA-2 single crystals. Chem Commun 51:11500–11503
20. Pérez-Mendoza M, Gonzalez J, Wright PA, Seaton NA (2004) Structure of the mesoporous silica SBA-2, determined by a percolation analysis of adsorption. Langmuir 20:9856–9860
21. Zhao D, Wan Y, Zhou W (2013) Representative Mesoporous Silica Molecular Sieves. Ordered Mesoporous Mater: 153–217. https://doi.org/10.1002/9783527647866.CH5
22. Sakamoto Y et al (2002) Three-Dimensional Cubic Mesoporous Structures of SBA-12 and Related Materials by Electron Crystallography. J Phys Chem B 106:3118–3123
23. Garcia-Bennett AE, Williamson S, Wright PA, Shannon IJ (2002) Control of structure, pore size and morphology of three-dimensionally ordered mesoporous silicas prepared using the dicationic surfactant [CH3(CH2)15N(CH3)2(CH2)3N(CH3)3]Br 2. J Mater Chem 12:3533–3540
24. Inagaki S, Guan S, Fukushima Y, Ohsuna T, Terasaki O (1999) Novel mesoporous materials with a uniform distribution of organic groups and inorganic oxide in their frameworks. J Am Chem Soc 121:9611–9614
25. Guan S, Inagaki S, Ohsuna T, Terasaki O (2000) Cubic hybrid organic-inorganic mesoporous crystal with a decaoctahedral shape [13]. J Am Chem Soc 122:5660–5661
26. Guan S, Inagaki S, Ohsuna T, Terasaki O (2001) Hybrid ethane–siloxane mesoporous materials with cubic symmetry. Microporous Mesoporous Mater 44–45:165–172
27. Dhepe PL, Fukuoka A, Ichikawa M (2003) Novel fabrication and catalysis of nano-structured Rh and RhPt alloy particles occluded in ordered mesoporous silica templates using supercritical carbon dioxide. Phys Chem Chem Phys 5:5565–5573
28. Kruk M, Jaroniec M, Guan S, Inagaki S (2000) Adsorption and Thermogravimetric Characterization of Mesoporous Materials with Uniform Organic−Inorganic Frameworks. J Phys Chem B 105:681–689
29. Fukuoka A et al (2006) Nanonecklaces of platinum and gold with high aspect ratios synthesized in mesoporous organosilica templates by wet hydrogen reduction. Chem Mater 18:337–343
30. Fukuoka A et al (2003) Palladium nanowires and nanoparticles in mesoporous silica templates. Inorganica Chim Acta 350:371–378
31. Ravikovitch PI, Neimark AV (2002) Density Functional Theory of Adsorption in Spherical Cavities and Pore Size Characterization of Templated Nanoporous Silicas with Cubic and Three-Dimensional Hexagonal Structures. Langmuir 18:1550–1560
32. Stöber W, Fink A, Bohn E (1968) Controlled growth of monodisperse silica spheres in the micron size range. J Colloid Interface Sci 26:62–69
33. Narayan R, Nayak UY, Raichur AM, Garg S (2018) Mesoporous silica nanoparticles: a comprehensive review on synthesis and recent advances. Pharmaceutics 10
34. Zhou Y et al (2018) Mesoporous silica nanoparticles for drug and gene delivery. Acta Pharm Sin B 8:165–177

35. Sol-Gel Science: The Physics and Chemistry of Sol-Gel Processing - C. Jeffrey Brinker, George W. Scherer - Google Books. https://www.sciencedirect.com/book/9780080571034/solgel-science#book-description
36. Manzano M, Vallet-Regí M (2020) Mesoporous silica nanoparticles for drug delivery. Adv Funct Mater 30
37. Cai Q et al (2001) Dilute solution routes to various controllable morphologies of MCM-41 silica with a basic medium. Chem Mater 13:258–263
38. Lai CY et al (2003) A mesoporous silica nanosphere-based carrier system with chemically removable CdS nanoparticle caps for stimuli-responsive controlled release of neurotransmitters and drug molecules. J Am Chem Soc 125:4451–4459
39. Yan Y et al (2019) Exploring the effect of porous structure on thermal conductivity in templated mesoporous silica films. J Phys Chem C 123:21721–21730
40. Yamamoto E, Kuroda K (2018) Preparation and controllability of mesoporous silica nanoparticles. Enzymes (Essen) 44:1–10
41. Cauda V, Argyo C, Piercey DG, Bein T (2011) 'Liquid-phase calcination' of colloidal mesoporous silica nanoparticles in high-boiling solvents. J Am Chem Soc 133:6484–6486
42. Kumar S, Malik MM, Purohit R (2017) Synthesis methods of mesoporous silica materials. Mater Today Proc 4:350–357
43. Hoffmann F, Cornelius M, Morell J, Fröba M (2006) Silica-based mesoporous organic-inorganic hybrid materials. Angew Chem Int Ed 45:3216–3251
44. Zhou Y, Schattka JH, Antonietti M (2004) Room-temperature ionic liquids as template to monolithic mesoporous silica with wormlike pores via a sol-gel nanocasting technique. Nano Lett 4:477–481
45. de Greñu BD, de los Reyes R, Costero AM, Amorós P, Ros-Lis JV (2020) Recent progress of microwave-assisted synthesis of silica materials. Nanomaterials 10:1092
46. Yao Y et al (2001) Encapsulation of fluorescein into MCM-41 mesoporous molecular sieve by a sol-gel method. Mater Lett 48:44–48
47. Bian S et al (2013) Organic/inorganic hybrid mesoporous silica membrane rapidly synthesized by a microwave-assisted method and its application in enzyme adsorption and electrocatalysis. J Mater Chem B 1:3267–3276
48. Evaporation-Induced Self-Assembly: Nanostructures Made Easy - Brinker - 1999 - Advanced Materials - Wiley Online Library. https://www.sciencedirect.com/topics/materials-science/evaporation-induced-self-assembly
49. Jing X et al (2020) Phosphate removal using free-standing functionalized mesoporous silica films with excellent recyclability. Microporous Mesoporous Mater 296:109953
50. Pal N, Lee JH, Cho EB (2020) Recent Trends in Morphology-Controlled Synthesis and Application of Mesoporous Silica Nanoparticles. Nanomaterials (Basel) 10:1–38
51. Chen Y et al (2010) Hollow/rattle-type mesoporous nanostructures by a structural difference-based selective etching strategy. ACS Nano 4:529–539
52 Walcarius A, Sibottier E, Etienne M, Ghanbaja J (2007) Electrochemically assisted self-assembly of mesoporous silica thin films. Nat Mater 6(8):602–608
53. Ding L, Su B (2015) An electrochemistry assisted approach for fast, low-cost and gram-scale synthesis of mesoporous silica nanoparticles. RSC Adv 5:65922–65926
54. Lakowicz JR (1983) Quenching of fluorescence. Principles of Fluorescence Spectroscopy: 257–301. https://doi.org/10.1007/978-1-4615-7658-7_9
55. Hide F et al (1996) Nanoscale Materials with Mesostructured Interiors**. Phys Rev B Condens Matter 273:27
56 Saad WS, Prud'Homme RK (2016) Principles of nanoparticle formation by flash nanoprecipitation. Nano Today 11:212–227
57. Fu Z et al (2020) Direct preparation of drug-loaded mesoporous silica nanoparticles by sequential flash nanoprecipitation. Chem Eng J 382:122905
58. Fuentes-García JA et al (2021) Effect of ultrasonic irradiation power on sonochemical synthesis of gold nanoparticles. Ultrason Sonochem 70:105274
59. El-Fiqi A, Bakry M (2020) Facile and rapid ultrasound-mediated synthesis of spherical mesoporous silica submicron particles with high surface area and worm-like mesoporosity. Mater Lett 281:128620
60. Porrang S, Rahemi N, Davaran S, Mahdavi M, Hassanzadeh B (2021) Preparation and in-vitro evaluation of mesoporous biogenic silica nanoparticles obtained from rice and wheat husk as a biocompatible carrier for anti-cancer drug delivery. Eur J Pharm Sci 163:105866
61. Porrang S, Rahemi N, Davaran S, Mahdavi M, Hassanzadeh B (2021) Synthesis of temperature/pH dual-responsive mesoporous silica nanoparticles by surface modification and radical polymerization for anti-cancer drug delivery. Colloids Surf A Physicochem Eng Asp 623:126719
62. Porrang S et al (2021) Direct surface modification of mesoporous silica nanoparticles by DBD plasma as a green approach to prepare dual-responsive drug delivery system. J Taiwan Inst Chem Eng 123:47–58
63. Li Z, Zhang Y, Feng N (2019) Mesoporous silica nanoparticles: synthesis, classification, drug loading, pharmacokinetics, biocompatibility, and application in drug delivery. 16:219–237. https://doi.org/10.1080/17425247.2019.1575806
64. Selvarajan V, Obuobi S, Ee PLR (2020) Silica Nanoparticles-A Versatile Tool for the Treatment of Bacterial Infections. Front Chem 8. https://doi.org/10.3389/fchem.2020.00602
65. Lin HP, Mou CY (2002) Structural and Morphological Control of Cationic Surfactant-Templated Mesoporous Silica. Acc Chem Res 35:927–935
66. (2000) Which surfactants reduce surface tension faster? A scaling argument for diffusion-controlled adsorption. Adv Colloid Interface Sci 85:61–97
67. Kumar M et al (2021) Influence of cationic surfactant cetyltrimethylammonium bromide for electrochemical detection of guanine, uric acid and dopamine. J Mol Liq 321:114893
68. Downing MA, Jain PK (2020) Mesoporous silica nanoparticles: synthesis, properties, and biomedical applications. Nanoparticles for Biomedical Applications: Fundamental Concepts, Biological Interactions and Clinical Applications: 267–281. https://doi.org/10.1016/B978-0-12-816662-8.00016-3
69. Carvalho GC et al (2022) Cetyltrimethylammonium bromide in the synthesis of mesoporous silica nanoparticles: General aspects and in vitro toxicity. Adv Colloid Interface Sci 307:102746
70. Che S et al (2003) A novel anionic surfactant templating route for synthesizing mesoporous silica with unique structure. Nat Mater 2003 2(12):801–805
71. Beck JS et al (1992) A new family of mesoporous molecular sieves prepared with liquid crystal templates. J Am Chem Soc 114:10834–10843
72. Kankala RK et al (2020) nanoarchitectured structure and surface biofunctionality of mesoporous silica nanoparticles. Adv Mater 32:1907035
73. Tanev PT, Pinnavaia TJ (1996) Mesoporous silica molecular sieves prepared by ionic and neutral surfactant templating : a comparison of physical properties. Chem Mater 8:2068–2079
74. Khodaee P, Najmoddin N, Shahrad S (2018) The effect of ethanol and temperature on the structural properties of mesoporous silica synthesized by the sol-gel method. 2018 25th Iranian Conference on Biomedical Engineering and 2018 3rd International Iranian Conference on Biomedical Engineering, ICBME 2018. https://doi.org/10.1109/ICBME.2018.8703594

75. Liu J, Yang Q, Zhao XS, Zhang L (2007) Pore size control of mesoporous silicas from mixtures of sodium silicate and TEOS. Microporous Mesoporous Mater 106:62–67
76. Niu D, Ma Z, Li Y, Shi J (2010) Synthesis of core-shell structured dual-mesoporous silica spheres with tunable pore size and controllable shell thickness. J Am Chem Soc 132:15144–15147
77. Yang J et al (2014) Boric acid assisted formation of mesostructured silica: from hollow spheres to hierarchical assembly. RSC Adv 4:20069–20076
78. Lebedev OI, Van Tendeloo G, Collart O, Cool P, Vansant EF (2004) Structure and microstructure of nanoscale mesoporous silica spheres. Solid State Sci 6:489–498
79 Ågren P et al (1999) Kinetics of cosurfactant−surfactant−silicate phase behavior. 1. short-chain alcohols. J Phys Chem B 103:5943–5948
80. Han L et al (2011) Anionic surfactants templating route for synthesizing silica hollow spheres with different shell porosity. Solid State Sci 13:721–728
81. Kleitz F, Marlow F, Stucky GD, Schüth F (2001) Mesoporous Silica Fibers: Synthesis, Internal Structure, and Growth Kinetics. Chem Mater 13:3587–3595
82. Isa EDM, Ahmad H, Rahman MBA (2019) Optimization of synthesis parameters of mesoporous silica nanoparticles based on ionic liquid by experimental design and its application as a drug delivery agent. J Nanomater 2019
83. Yu J, Shi JL, Chen HR, Yan JN, Yan DS (2001) Effect of inorganic salt addition during synthesis on pore structure and hydrothermal stability of mesoporous silica. Microporous Mesoporous Mater 46:153–162
84. Luechinger M, Pirngruber GD, Lindlar B, Laggner P, Prins R (2005) The effect of the hydrophobicity of aromatic swelling agents on pore size and shape of mesoporous silicas. Microporous Mesoporous Mater 79:41–52
85 Kresge CT, Leonowicz ME, Roth WJ, Vartuli JC, Beck JS (1992) Ordered mesoporous molecular sieves synthesized by a liquid-crystal template mechanism. Nature 359(6397):710–712
86. Cauda V, Schlossbauer A, Kecht J, Zürner A, Bein T (2009) Multiple core-shell functionalized colloidal mesoporous silica nanoparticles. J Am Chem Soc 131:11361–11370
87. Urata C, Aoyama Y, Tonegawa A, Yamauchi Y, Kuroda K (2009) Dialysis process for the removal of surfactants to form colloidal mesoporous silica nanoparticles. Chem Commun: 5094–5096. https://doi.org/10.1039/B908625K
88. Hitz S, Prins R (1997) Influence of template extraction on structure, activity, and stability of MCM-41 catalysts. J Catal 168:194–206
89. Yang CM, Zibrowius B, Schmidt W, Schüth F (2004) Stepwise removal of the copolymer template from mesopores and micropores in SBA-15. Chem Mater 16:2918–2925
90. Kang H et al (2010) Preparation of silica-sustained electrospun polyvinylpyrrolidone fibers with uniform mesopores via oxidative removal of template molecules by H2O2 treatment. Mater Res Bull 45:830–837
91. Kecht J, Bein T (2008) Oxidative removal of template molecules and organic functionalities in mesoporous silica nanoparticles by H2O2 treatment. Microporous Mesoporous Mater 116:123–130
92. Florin E, Kjellander R, Eriksson JC (1984) Salt effects on the cloud point of the poly(ethylene oxide)+ water system. J Chem Soc Faraday Trans 1: Phys Chem Condens Phases. 80:2889–2910
93. Büchel G, Denoyel R, Llewellyn PL, Rouquerol J (2001) In situ surfactant removal from MCM-type mesostructures by ozone treatment. J Mater Chem 11:589–593
94. Wang HC et al (2010) Low temperature strategy to synthesize high surface area mesoporous hydroxypropyl-β-cyclodextrin-based silicas via benign template removal. Microporous Mesoporous Mater 134:175–180
95. Lu AH, Li WC, Schmidt W, Schüth F (2006) Low temperature oxidative template removal from SBA-15 using MnO4− solution and carbon replication of the mesoporous silica product. J Mater Chem 16:3396–3401
96. Naik SP, Elangovan SP, Okubo T, Sokolov I (2007) Morphology Control of Mesoporous Silica Particles. J Phys Chem C 111:11168–11173
97. Han L et al (2013) One-pot morphology-controlled synthesis of various shaped mesoporous silica nanoparticles. J Mater Sci 48:5718–5726
98. Zhang H et al (2006) Engineered complex emulsion system: Toward modulating the pore length and morphological architecture of mesoporous silicas. J Phys Chem B 110:25908–25915
99. Maleki A et al (2017) Mesoporous silica materials: From physico-chemical properties to enhanced dissolution of poorly water-soluble drugs. J Control Release 262:329–347
100. Horcajada P, Rámila A, Pérez-Pariente J, Vallet-Regí M (2004) Influence of pore size of MCM-41 matrices on drug delivery rate. Microporous Mesoporous Mater 68:105–109
101. Varga N et al (2015) Mesoporous silica core–shell composite functionalized with polyelectrolytes for drug delivery. Microporous Mesoporous Mater 213:134–141
102. Wang Y et al (2015) Mesoporous silica nanoparticles in drug delivery and biomedical applications. Nanomedicine 11:313–327
103. Jana SK, Mochizuki A, Namba S (2004) Progress in pore-size control of mesoporous MCM-41 molecular sieve using surfactant having different alkyl chain lengths and various organic auxiliary chemicals. Catal Surv Asia 8:1–13
104. Zhang L et al (2008) Fabrication and Size-Selective Bioseparation of Magnetic Silica Nanospheres with Highly Ordered Periodic Mesostructure. Adv Funct Mater 18:3203–3212
105. Widenmeyer M, Anwander R (2002) Pore Size Control of Highly Ordered Mesoporous Silica MCM-48. Chem Mater 14:1827–1831
106. Vallet-Regi M, Rámila A, Del Real RP, Pérez-Pariente J (2001) A new property of MCM-41: Drug delivery system. Chem Mater 13:308–311
107. Vallet-Regí M, Colilla M, Manzano M (2008) Recent advances in ceramic implants as drug delivery systems for biomedical applications. Int J Nanomedicine 3:403
108. Manzano M, Vallet-Regí M (2010) New developments in ordered mesoporous materials for drug delivery. J Mater Chem 20:5593–5604
109. Argyo C, Weiss V, Bräuchle C, Bein T (2014) Multifunctional mesoporous silica nanoparticles as a universal platform for drug delivery. Chem Mater 26:435–451
110. Knežević N, Durand JO (2015) Large pore mesoporous silica nanomaterials for application in delivery of biomolecules. Nanoscale 7:2199–2209
111. Balas F, Manzano M, Horcajada P, Vallet-Regi M (2006) Confinement and controlled release of bisphosphonates on ordered mesoporous silica-based materials. J Am Chem Soc 128:8116–8117
112. Chiang YD et al (2011) Controlling particle size and structural properties of mesoporous silica nanoparticles using the taguchi method. J Phys Chem C 115:13158–13165
113. Wu KCW, Yamauchi Y (2011) Controlling physical features of mesoporous silica nanoparticles (MSNs) for emerging applications. J Mater Chem 22:1251–1256
114. Lee CH et al (2010) Intracellular pH-responsive mesoporous silica nanoparticles for the controlled release of anticancer chemotherapeutics. Angew Chem Int Ed Engl 49:8214–8219
115. Huang X, Teng X, Chen D, Tang F, He J (2010) The effect of the shape of mesoporous silica nanoparticles on cellular uptake and cell function. Biomaterials 31:438–448
116. Huang X et al (2011) The shape effect of mesoporous silica nanoparticles on biodistribution, clearance, and biocompatibility in vivo. ACS Nano 5:5390–5399

117. Ma K, Sai H, Wiesner U (2012) Ultrasmall sub-10 nm near-infrared fluorescent mesoporous silica nanoparticles. J Am Chem Soc 134:13180–13183
118. He Q, Cui X, Cui F, Guo L, Shi J (2009) Size-controlled synthesis of monodispersed mesoporous silica nano-spheres under a neutral condition. Microporous Mesoporous Mater 117:609–616
119. Yu M et al (2012) A simple approach to prepare monodisperse mesoporous silica nanospheres with adjustable sizes. J Colloid Interface Sci 376:67–75
120. Jin H et al (2006) Control of Morphology and Helicity of Chiral Mesoporous Silica. Adv Mater 18:593–596
121. Ozin GA, Chomski E, Khushalani D, MacLachlan MJ (1998) Mesochemistry. Curr Opin Colloid Interface Sci 3:181–193
122. Aquib M et al (2019) Targeted and stimuli–responsive mesoporous silica nanoparticles for drug delivery and theranostic use. J Biomed Mater Res A 107:2643–2666
123. Kecht J, Schlossbauer A, Bein T (2008) Selective functionalization of the outer and inner surfaces in mesoporous silica nanoparticles. Chem Mater 20:7207–7214
124 Hoang Thi TT et al (2019) Functionalized mesoporous silica nanoparticles and biomedical applications. Mater Sci Eng C 99:631–656
125. Zaharudin NS, Mohamed Isa ED, Ahmad H, Abdul Rahman MB, Jumbri K (2020) Functionalized mesoporous silica nanoparticles templated by pyridinium ionic liquid for hydrophilic and hydrophobic drug release application. J Saudi Chem Soc 24:289–302
126. Rastegari E et al (2021) An update on mesoporous silica nanoparticle applications in nanomedicine. Pharmaceutics 13
127. Elbialy NS, Aboushoushah SF, Sofi BF, Noorwali A (2020) Multifunctional curcumin-loaded mesoporous silica nanoparticles for cancer chemoprevention and therapy. Microporous Mesoporous Mater 291:109540
128. Liu X et al (2016) In vitro and in vivo evaluation of puerarin-loaded PEGylated mesoporous silica nanoparticles. 42:2031–2037. https://doi.org/10.1080/03639045.2016.1190742
129. Lin J et al (2018) PEGylated lipid bilayer coated mesoporous silica nanoparticles for co-delivery of paclitaxel and curcumin: design, characterization and its cytotoxic effect. Int J Pharm 536:272–282
130. Morales-Cruz M et al (2019) Smart Targeting To Improve Cancer Therapeutics. Drug Des Devel Ther 13:3753–3772
131. Ji Y et al (2021) Facile fabrication of nanocarriers with yolk-shell mesoporous silica nanoparticles for effective drug delivery. J Drug Deliv Sci Technol 63:102531
132. Zhao Y, Vivero-Escoto JL, Slowing II, Trewyn BG, Lin VSY (2010) Capped mesoporous silica nanoparticles as stimuli-responsive controlled release systems for intracellular drug/gene delivery. 7:1013–1029. https://doi.org/10.1517/17425247.2010.498816
133. Rahikkala A et al (2018) Mesoporous Silica Nanoparticles for Targeted and Stimuli-Responsive Delivery of Chemotherapeutics: A Review. Adv Biosyst 2:1800020
134. Sun X, Agate S, Salem KS, Lucia L, Pal L (2021) Hydrogel-Based Sensor Networks: Compositions, Properties, and Applications - A Review. ACS Appl Bio Mater 4:140–162
135. Shakeran Z, Keyhanfar M, Varshosaz J, Sutherland DS (2021) Biodegradable nanocarriers based on chitosan-modified mesoporous silica nanoparticles for delivery of methotrexate for application in breast cancer treatment. Mater Sci Eng C 118:111526
136. Wagner J et al (2021) Mesoporous Silica Nanoparticles as pH-Responsive Carrier for the Immune-Activating Drug Resiquimod Enhance the Local Immune Response in Mice. ACS Nano 15:4450–4466
137. Kesse S et al (2019) Mesoporous silica nanomaterials: versatile nanocarriers for cancer theranostics and drug and gene delivery. Pharmaceutics 11:77
138. Narayanankutty A, Job JT, Narayanankutty V (2019) Glutathione, an antioxidant tripeptide: dual roles in carcinogenesis and chemoprevention. Curr Protein Pept Sci 20:907–917
139. Niu B et al (2021) Application of glutathione depletion in cancer therapy: Enhanced ROS-based therapy, ferroptosis, and chemotherapy. Biomaterials 277:121110
140. Gisbert-Garzarán M, Vallet-Regí M (2021) Redox-responsive mesoporous silica nanoparticles for cancer treatment: recent updates. Nanomaterials (Basel) 11
141. Daund V, Chalke S, Sherje AP, Kale PP (2021) ROS responsive mesoporous silica nanoparticles for smart drug delivery: A review. J Drug Deliv Sci Technol 64:102599
142. Chen L et al (2016) Multifunctional redox-responsive mesoporous silica nanoparticles for efficient targeting drug delivery and magnetic resonance imaging. ACS Appl Mater Interfaces 8:33829–33841
143. Liu M et al (2020) Paclitaxel and quercetin co-loaded functional mesoporous silica nanoparticles overcoming multidrug resistance in breast cancer. Colloids Surf B Biointerfaces 196:111284
144. Zhao S et al (2017) A redox-responsive strategy using mesoporous silica nanoparticles for co-delivery of siRNA and doxorubicin. J Mater Chem B 5:6908–6919
145. Chen M et al (2020) Targeted and redox-responsive drug delivery systems based on carbonic anhydrase IX-decorated mesoporous silica nanoparticles for cancer therapy. Sci Rep 10(1):1–12
146. Luo Z et al. Drug Delivery Mesoporous Silica Nanoparticles End-Capped with Collagen: Redox-Responsive Nanoreservoirs for Targeted Drug Delivery** Zuschriften. https://doi.org/10.1002/ange.201005061
147. Kundu M et al (2021) In vivo therapeutic evaluation of a novel bis-lawsone derivative against tumor following delivery using mesoporous silica nanoparticle based redox-responsive drug delivery system. Mater Sci Eng C Mater Biol Appl 126
148. Li M, Zhao G, Su WK, Shuai Q (2020) Enzyme-Responsive Nanoparticles for Anti-tumor Drug Delivery. Front Chem 8:647
149. Kumar B et al (2017) Mesoporous silica nanoparticle based enzyme responsive system for colon specific drug delivery through guar gum capping. Colloids Surf B Biointerfaces 150:352–361
150. Vaghasiya K, Ray E, Sharma A, Katare OP, Verma RK (2020) Matrix metalloproteinase-responsive mesoporous silica nanoparticles cloaked with cleavable protein for 'self-actuating' on-demand controlled drug delivery for cancer therapy. ACS Appl Bio Mater 3:4987–4999
151. Lin SY (2020) Thermoresponsive gating membranes embedded with liquid crystal(s) for pulsatile transdermal drug delivery: An overview and perspectives. J Control Release 319:450–474
152 Wang K, Liu Q, Liu G, Zeng Y (2020) Novel thermoresponsive homopolymers of poly[oligo(ethylene glycol) (acyloxy) methacrylate]s: LCST-type transition in water and UCST-type transition in alcohols. Polymer (Guildf) 203:122746
153. Ugazio E et al (2016) Thermoresponsive mesoporous silica nanoparticles as a carrier for skin delivery of quercetin. Int J Pharm 511:446–454
154. Zhu J et al (2021) Reactive Oxygen Species Scavenging Sutures for Enhanced Wound Sealing and Repair. Small Struct 2:2100002
155. Shen Y et al (2018) ROS responsive resveratrol delivery from LDLR peptide conjugated PLA-coated mesoporous silica nanoparticles across the blood-brain barrier. J Nanobiotechnology 16:1–17

156. Li J et al (2020) Reactive oxygen species-sensitive thioketal-linked mesoporous silica nanoparticles as drug carrier for effective antibacterial activity. Mater Des 195:109021
157. Farzin A, Etesami SA, Quint J, Memic A, Tamayol A (2020) Magnetic Nanoparticles in Cancer Therapy and Diagnosis. Adv Healthc Mater 9:1901058
158. Sampath Udeni Gunathilake TM, Ching YC, Chuah CH, Rahman NA, Liou NS (2020) Recent advances in celluloses and their hybrids for stimuli-responsive drug delivery. Int J Biol Macromol 158:670–688
159. Asgari M, Soleymani M, Miri T, Barati A (2021) Design of thermosensitive polymer-coated magnetic mesoporous silica nanocomposites with a core-shell-shell structure as a magnetic/temperature dual-responsive drug delivery vehicle. Polym Adv Technol 32:4101–4109
160. Peralta ME et al (2019) Synthesis and in vitro testing of thermoresponsive polymer-grafted core-shell magnetic mesoporous silica nanoparticles for efficient controlled and targeted drug delivery. J Colloid Interface Sci 544:198–205
161. Lin FC, Xie Y, Deng T, Zink JI (2021) Magnetism, Ultrasound, and Light-Stimulated Mesoporous Silica Nanocarriers for Theranostics and beyond. J Am Chem Soc 143:6025–6036
162 Entzian K, Aigner A (2021) Drug delivery by ultrasound-responsive nanocarriers for cancer treatment. Pharmaceutics 13:1135
163. Li X, Wang Z, Xia H (2019) Ultrasound reversible response nanocarrier based on sodium alginate modified mesoporous silica nanoparticles. Front Chem 7:59
164. Rapp TL, DeForest CA (2021) Targeting drug delivery with light: A highly focused approach. Adv Drug Deliv Rev 171:94–107
165. Qi RQ et al (2020) Development of local anesthetic drug delivery system by administration of organo-silica nanoformulations under ultrasound stimuli: in vitro and in vivo investigations. 28:54–62. https://doi.org/10.1080/10717544.2020.1856220
166. Qin Y et al (2021) Novel photothermal-responsive sandwich-structured mesoporous silica nanoparticles: synthesis, characterization, and application for controlled drug delivery. J Mater Sci 56:12412–12422
167. Deng J, Walther A (2020) ATP-Responsive and ATP-Fueled Self-Assembling Systems and Materials. Adv Mater 32:2002629
168. Zheng FF et al (2015) Aptamer/Graphene Quantum Dots Nanocomposite Capped Fluorescent Mesoporous Silica Nanoparticles for Intracellular Drug Delivery and Real-Time Monitoring of Drug Release. Anal Chem 87:11739–11745
169. Zhu CL, Lu CH, Song XY, Yang HH, Wang XR (2011) Bioresponsive controlled release using mesoporous silica nanoparticles capped with aptamer-based molecular gate. J Am Chem Soc 133:1278–1281
170. Li X et al (2021) Research progress of response strategies based on tumor microenvironment in drug delivery systems. J Nanopart Res 23:1–14
171. Li F, Zhu Y, Wang Y (2014) Dual-responsive drug delivery system with real time tunable release behavior. Microporous Mesoporous Mater 200:46–51
172. Zhao P et al (2014) A study of chitosan hydrogel with embedded mesoporous silica nanoparticles loaded by ibuprofen as a dual stimuli-responsive drug release system for surface coating of titanium implants. Colloids Surf B Biointerfaces 123:657–663
173. Zhu Y et al (2010) Dipolar molecules as impellers achieving electric-field-stimulated release. J Am Chem Soc 132:1450–1451
174. García-Fernández A et al (2020) Electro-responsive films containing voltage responsive gated mesoporous silica nanoparticles grafted onto PEDOT-based conducting polymer. J Control Release 323:421–430
175. Hou L et al (2018) Self-Regulated Carboxyphenylboronic Acid-Modified Mesoporous Silica Nanoparticles with 'touch Switch' Releasing Property for Insulin Delivery. ACS Appl Mater Interfaces 10:21927–21938
176. Huang Q et al (2021) Synthesis and testing of polymer grafted mesoporous silica as glucose-responsive insulin release drug delivery systems. Eur Polym J 157:110651
177. Sabir N, Hussain T, Mangi MH, Zhao D, Zhou X (2019) Matrix metalloproteinases: Expression, regulation and role in the immunopathology of tuberculosis. Cell Prolif 52:e12649
178. Zhang B et al (2021) Macrophage-mediated degradable gelatin-coated mesoporous silica nanoparticles carrying pirfenidone for the treatment of rat spinal cord injury. Nanomedicine 37:102420
179. Cheng Q et al (2019) Dual stimuli-responsive bispillar[5]arene-based nanoparticles for precisely selective drug delivery in cancer cells. Chem Commun 55:2340–2343
180. Policastro LL, Ibañez IL, Notcovich C, Duran HA, Podhajcer OL (2013) the tumor microenvironment: characterization, redox considerations, and novel approaches for reactive oxygen species-targeted gene therapy. Antioxid Redox Signal 19:854–895. https://pubmed.ncbi.nlm.nih.gov/22794113/
181. Thapa R et al (2023) Unlocking the potential of mesoporous silica nanoparticles in breast cancer treatment. J Nanopart Res 25(8):1–28
182. Du J et al (2021) Polydopamine/keratin complexes as gatekeepers of mesoporous silica nanoparticles for pH and GSH dual responsive drug delivery. Mater Lett 293:129676
183. Wang Y et al (2021) PH/H2O2 dual-responsive chiral mesoporous silica nanorods coated with a biocompatible active targeting ligand for cancer therapy. ACS Appl Mater Interfaces 13:35397–35409
184. Wen J et al (2016) Construction of a triple-stimuli-responsive system based on cerium oxide coated mesoporous silica nanoparticles. Sci Rep 6(1):1–10
185. Liu X et al (2016) Irinotecan Delivery by Lipid-Coated Mesoporous Silica Nanoparticles Shows Improved Efficacy and Safety over Liposomes for Pancreatic Cancer. ACS Nano 10:2702–2715
186. Li X, Chen M, Zhao Y, Sun L (2021) Redox/pH/NIR-responsive degradable silica nanospheres with fluorescence for drug release and photothermal therapy. Biochem Eng J 168:107955
187. Feng Y et al (2019) Thermo- and pH-responsive, Lipid-coated, mesoporous silica nanoparticle-based dual drug delivery system to improve the antitumor effect of hydrophobic drugs. Mol Pharm 16:422–436
188. Chen X, Liu Z (2016) Dual responsive mesoporous silica nanoparticles for targeted co-delivery of hydrophobic and hydrophilic anticancer drugs to tumor cells. J Mater Chem B 4:4382–4388
189. Fei Y et al (2020) Hierarchical integration of degradable mesoporous silica nanoreservoirs and supramolecular dendrimer complex as a general-purpose tumor-targeted biomimetic nanoplatform for gene/small-molecule anticancer drug co-delivery. Nanoscale 12:16102–16112
190. Xu L et al (2022) Dual drug release mechanisms through mesoporous silica nanoparticle/electrospun nanofiber for enhanced anticancer efficiency of curcumin. J Biomed Mater Res A 110:316–330
191. Samadzadeh S, Babazadeh M, Zarghami N, Pilehvar-Soltanahmadi Y, Mousazadeh H (2021) An implantable smart hyperthermia nanofiber with switchable, controlled and sustained drug release: Possible application in prevention of cancer local recurrence. Mater Sci Eng C 118:111384
192. Yu Q, Deng T, Lin FC, Zhang B, Zink JI (2020) Supramolecular Assemblies of Heterogeneous Mesoporous Silica Nanoparticles to

Co-deliver Antimicrobial Peptides and Antibiotics for Synergistic Eradication of Pathogenic Biofilms. ACS Nano 14:5926–5937
193. Babaei M et al (2020) Targeted rod-shaped mesoporous silica nanoparticles for the co-delivery of camptothecin and survivin shRNA in to colon adenocarcinoma in vitro and in vivo. Eur J Pharm Biopharm 156:84–96
194. Li Y et al (2020) Hydroxychloroquine-loaded hollow mesoporous silica nanoparticles for enhanced autophagy inhibition and radiation therapy. J Control Release 325:100–110
195. Cao Y et al (2020) Folate functionalized pH-sensitive photothermal therapy traceable hollow mesoporous silica nanoparticles as a targeted drug carrier to improve the antitumor effect of doxorubicin in the hepatoma cell line SMMC-7721. 27:258–268. https://doi.org/10.1080/10717544.2020.1718801
196. Ahmed H et al (2022) Biomedical applications of mesoporous silica nanoparticles as a drug delivery carrier. J Drug Deliv Sci Technol 76:103729
197. Li H, Granados A, Fernández E, Pleixats R, Vallribera A (2020) Anti-inflammatory Cotton Fabrics and Silica Nanoparticles with Potential Topical Medical Applications. ACS Appl Mater Interfaces 12:25658–25675
198. Cha BG, Kim J (2019) Functional mesoporous silica nanoparticles for bio-imaging applications. Wiley Interdiscip Rev Nanomed Nanobiotechnol 11
199. He Z et al (2020) Red aggregation-induced emission luminogen and Gd3+ codoped mesoporous silica nanoparticles as dual-mode probes for fluorescent and magnetic resonance imaging. J Colloid Interface Sci 567:136–144
200. Er O et al (2020) Radiolabeling, in vitro cell uptake, and in vivo photodynamic therapy potential of targeted mesoporous silica nanoparticles containing zinc phthalocyanine. Mol Pharm 17:2648–2659
201. Eguílaz M, Villalonga R, Rivas G (2018) Electrochemical biointerfaces based on carbon nanotubes-mesoporous silica hybrid material: Bioelectrocatalysis of hemoglobin and biosensing applications. Biosens Bioelectron 111:144–151
202. Jafari S et al (2019) Mesoporous silica nanoparticles for therapeutic/diagnostic applications. Biomed Pharmacother 109:1100–1111
203. Ge S et al (2017) Ultrasensitive photoelectrochemical biosensing of cell surface n-glycan expression based on the enhancement of nanogold-assembled mesoporous silica amplified by graphene quantum dots and hybridization chain reaction. ACS Appl Mater Interfaces 9:6670–6678
204. Chen ZZ et al (2016) Memantine mediates neuroprotection via regulating neurovascular unit in a mouse model of focal cerebral ischemia. Life Sci 150:8–14
205. Jimenez-Falcao S et al (2019) Avidin-gated mesoporous silica nanoparticles for signal amplification in electrochemical biosensor. Electrochem commun 108:106556
206. Chen L, Zhou X, He C (2019) Mesoporous silica nanoparticles for tissue-engineering applications. Wiley Interdiscip Rev Nanomed Nanobiotechnol 11
207. Yousefiasl S et al (2022) Chitosan/alginate bionanocomposites adorned with mesoporous silica nanoparticles for bone tissue engineering. J Nanostructure Chem 1–15. https://doi.org/10.1007/S40097-022-00507-Z/METRICS